



Calhoun: The NPS Institutional Archive
DSpace Repository

Theses and Dissertations

1. Thesis and Dissertation Collection, all items

1969

Finite deflections of impulsively loaded, rigid
rectangular mild steel plates with two edges clamped.

Griffin, Robert Noble

Massachusetts Institute of Technology

<http://hdl.handle.net/10945/12218>

Downloaded from NPS Archive: Calhoun



Calhoun is the Naval Postgraduate School's public access digital repository for research materials and institutional publications created by the NPS community. Calhoun is named for Professor of Mathematics Guy K. Calhoun, NPS's first appointed -- and published -- scholarly author.

Dudley Knox Library / Naval Postgraduate School
411 Dyer Road / 1 University Circle
Monterey, California USA 93943

<http://www.nps.edu/library>

NPS ARCHIVE
1969
GRIFFIN, R.

FINITE DEFLECTIONS OF IMPULSIVELY
LOADED, RIGID RECTANGULAR MILD STEEL
PLATES WITH TWO EDGES CLAMPED

by

Robert Noble Griffin

Thesis Supervisor

Norman Jones

Thesis
G783

41320
10/11/11 10311 ROUTE 57100
MONTREY, CALIF. 93940

FINITE DEFLECTIONS OF IMPULSIVELY LOADED,
RIGID RECTANGULAR MILD STEEL PLATES
WITH TWO EDGES CLAMPED

by

ROBERT NOBLE GRIFFIN
Lieutenant, United States Navy

B.S., United States Naval Academy
(1960)

SUBMITTED IN PARTIAL FULFILLMENT
OF THE REQUIREMENTS FOR THE
DEGREE OF MASTER OF SCIENCE
IN NAVAL ARCHITECTURE AND
MARINE ENGINEERING
AND THE PROFESSIONAL DEGREE OF
NAVAL ENGINEER

at the

MASSACHUSETTS INSTITUTE OF
TECHNOLOGY

June, 1969

NPS ARCHIVE

1969

GRIFFIN, R.

~~Thesis~~
~~G-183~~

81
1969
414

TABLE OF CONTENTS

	Page
I. Introduction	1
II. Experimental Arrangement	2
Figure 1 - Arrangement Drawing	9
Figure 2 - Specimen Drawing	9
Figure 3 - Head Drawing	10
III. Discussion of Results	5
Table 1 - Results	11
Figure 4 - Graph	12
Figure 5 - Graph	13
Figure 6 - Graph	14
Figure 7 - Figure 6 Explanation	15
Graphs of Deflections	
Figure 8)- Specimen 6	16
Figure 9)-	17
Figure 10)- Specimen 7	18
Figure 11)-	19
Figure 12)- Specimen 12	20
Figure 13)-	21
Figure 14)- Specimen 14	22
Figure 15)-	23
Figure 16)- Specimen 20	24
Figure 17)-	25
Figure 18)- Specimen 28	26
Figure 19)-	27
IV. Conclusions	7

APPENDICES

	Page
A. Specimen Chemical Composition Table 2	28
B. Tensile Test Results Figure 19a Figure 20 Figure 21	29
C. Specimen Density Table 3	33
D. Pendulum Windage Loss Table 4 Figure 22	34
E. Strain Gage Results Table 5	37
F. Blast Chamber Firing Circuit Figure 23 Figure 24 Figure 25	40
G. Specimen Origin Plans Figure 26 Figure 27 Figure 28	
H. Initial Velocity Calculation	47

I. INTRODUCTION

The behavior of simple structures subject to large dynamic loads has received much attention in the past two decades. In general, the focus of attention has been on flat beams and circular plates. Some of the important theoretical developments in this area have been made by Symonds and Mentel [1]¹ for clamped beams; Bodner and Symonds [2] for cantilever beams; and Jones [3] for circular plates. Paralleling the theoretical work, experimentation has been conducted by Humphreys [4]; Florence and Firth [5] and Jones [6].

As yet, little work, either theoretical or experimental, has been accomplished for the rectangular plate. Inasmuch as the rectangular plate is an important component of any ship hull, a better understanding of the action of a plate under a dynamic load could lead to improvements in ship design.

Due to the time available, a complete study of plate configurations and materials was infeasible. Consequently, the parameters of the tests were limited to allow a fairly extensive study for the material, boundary conditions, and aspect ratio chosen. The test variables were plate loading and plate thickness.

The results of the experimentation should provide some insight into the dynamic behavior of rectangular plates. Of

¹Numbers in brackets designate References listed at the end of the paper.

value also is the comparison with beam theory and beam test results which show the proximity of beam and plate behavior under similar conditions.

II. EXPERIMENTAL ARRANGEMENT

A ballistic pendulum, as shown in Figure 1, served to measure the impulsive loading of the plates. The pendulum was constructed from a two foot piece of steel I-beam with a one-half inch steel plate welded on one end. The clamp or head which held the specimen was then bolted to the plate. On the other end of the I-beam was a lead balance weight and a terminal block. The terminal block held a .005 inch diameter tungsten wire and capillary wires which connected the pen (tungsten wire) to three $1\frac{1}{2}$ volt dry cell batteries. The pen barely touched the heat sensitive paper that was taped to the steel arc or track below the pendulum. The paper recorded the swing of the pendulum.

The plate specimens, shown in Figure 2, were cut from three thicknesses of hot, rolled, mild steel plate. The properties and composition of the steel are given in the Appendices. The samples were then milled to parallel the sides at three inches wide. The next step was to grind the specimens to an even thickness which removed the surface scale. Lastly, the plate surface was smoothed with very fine emery paper.

To protect the specimens from spalling, one-eighth inch neoprene was used at first. The neoprene was satisfactory; however, the explosive was so powerful that a good range of

deflections could not be attained with the thinner plates. Using one-half inch sponge rubber (hereafter referred to as foam) resulted in less impulse on the plate for the same thickness of explosive. It should be noted that Florence and Firth [5] used neoprene while Humphreys [4] used foam for the same type of experiments. Other than a difference in impulse there was no noticeable effect on the results from using the different materials.

The impulsive loads on the specimens were provided by Dupont Detasheet D. which is a flexible explosive. It was purchased in .010 and .015 inch thick sheets. After both the explosive and foam were cut to the same size as the plate being tested, the foam was coated with a layer of electrical tape. The foam was then glued to the plate, and the explosive was glued to the foam using rubber cement. Other than a slight softening of the detasheet there seemed to be no additional effect from the glue.

Actuating the explosive on the plate was achieved with a Dupont #6 electric blasting cap and a 12 to 20 inch long, one-eighth inch wide detasheet leader. Pressing the end of the leader into the explosive on the plate with a finger proved to be the best method of attaching the leader. Tests were conducted which determined that the explosive force of the detonator had no apparent effect on the pendulum. The tests simulated a normal experiment without the explosive on the plate. The end of the leader was held to the plate with a piece of tape. There was no effect as long as a metal

shield was placed between the detonator and pendulum and the leader was pulled tight. Thus, it led directly away from the specimen. Figure 3 shows the detonator and leader arrangement.

The leader arrangement was changed twice during the course of the experiment attempting to find the best way to achieve instantaneous uniform loading of the plate. In the first trial, a single leader was attached to the middle of the plate at one edge. After the samples showed deflections in which one side was higher than the other, a leader with three fingers on the end was tested. With this method, the equal length fingers at the end of the leader were attached across the plate centerline, at each side and in the middle. In this situation the thin specimens exhibited ripple-like deflections (Figure 16).

The remainder and greatest portion of the tests were completed using a single leader attached at the exact center of the plate. It was interesting to note that non-symmetric and ripple-like deflections were still produced even when the center leader was employed.

Achieving the proper boundary conditions was most difficult in that the samples slipped in the clamps. To prevent this occurrence during large deflections, it was necessary to cut teeth in the clamps. The teeth were then case hardened. In addition, high strength bolts were resorted to in order that a maximum amount of pressure could be applied to the clamps. These bolts were placed as closely together as practical. Figure 3 is a sketch of the head with a specimen.

III. DISCUSSION OF RESULTS

Table 1 contains a summary of plate properties, test results and test data. The final deflections of the plates assumed varying shapes which seemed to be a function of plate thickness. Therefore, two representative specimens of each thickness were graphed in Figures 8 through 19. A look at the plots will show the salient features of the types of deflections produced.

Specimen 6 as shown in Figures 8 and 9 is one of the thick (.173 inch) samples. All of the thick samples had the same type of deflections across the centerline. That is, across the middle of the plate ($X=0$) the deflections were concave. Specimen 28, Figure 18, shows the same, whereas at $X=1\frac{1}{2}$ there is a convex portion near the centerline. Longitudinally the deflections were nearly symmetrical and therefore only one-half the line was plotted in Figures 9 and 19.

The medium thickness plates (.0988 inch) begin to show the ripple effect mentioned earlier. In figures 10 through 13 there appear to be waves in both the transverse and longitudinal directions. This is particularly evident in Specimen 12. This sample is also an example of the effect of using a side-attached leader. As in the previous specimens, the plate deflections were nearly symmetrical longitudinally.

In the thinnest plates (.0642 inch), Figures 14 through 17, the ripple effect is most apparent. And there appears to be a set pattern to the waves as the ratio W/T is increased. For instance, the small convex section in the middle of the

$X = 1\frac{1}{2}$ line of Specimen 6 is more noticeable in Specimen 7 and is fully developed in Specimen 14. Specimen 6 had a side-attached leader while 7 and 14 had center-attached leaders.

Regardless of what type leader was used most specimens deflected with one edge higher than the other. In some cases, such as Specimen 12, this effect was enhanced by attaching the leader at the side of the plate. It was therefore decided to use the maximum deflection along the longitudinal center-line of the plates for theoretical comparisons as well as for plotting the results. The reason for so doing was to insure that all the readings compared would be taken at the same location. It was also believed that the plate center would be less effected by non-uniform loading.

Three graphs were plotted to evaluate the results. The first, Figure 4, is a comparison of non-dimensional deflection (W_c/T) with initial velocity. The graph shows an almost linear relationship between the variables for each plate thickness. Also, the slope of the line increases with decreasing thickness.

In Figure 5 thickness is constant. The purpose of the graph is to show the effect of aspect ratio (L/X) on the specimen deflection for a given impulse per unit area. The results of the two square plates, the one inch and the two inch flat beams all plot along the same line as the rectangular plates.

Since the beam tests were too few in number to produce conclusive results, the plate deflections were compared with beam theory and other experimental work in Figure 6. The plate results also fall close to the theoretical curves

developed for clamped beams by Jones [7] . In order to obtain the curves, the analysis had to be approximate and simplified. Yet they appear to be good engineering predictions of the results obtained for rectangular plates.

Other facts about the results are: (1) The deflections were not corrected for end rotation; the effect of which would be to increase the maximum deflection for positive angles and decrease the maximum deflection for negative angles. The error is considered small. (2) The end angles varied with plate thickness. The thinnest plate had positive rotations of about nine minutes. The middle thickness rotated hardly at all, while the thickest plate had negative rotations of about eight minutes. (3) Because rolled steel is sometimes stronger in one direction than another, the results were investigated to see if there was a difference between samples cut in different directions. There appeared to be none.

Additional specimen data and sample calculations are presented in the Appendices.

IV. CONCLUSIONS

The following conclusions are for mild steel plates with two edges rigidly clamped and the other edges free:

- (1) Rigid-plastic beam theory of large deflection with consideration of rate effects can be used to predict the deflection of rectangular plates subject to dynamic loads.
- (2) The waves in the plates are not wholly the result of the leader attachment.

- (3) Aspect ratio L/X has little effect on the maximum deflection of a plate for a given impulse per unit area.
- (4) The non-symmetry of deflections in some plates could have been caused by non-homogeneous plates or non-uniform explosives.

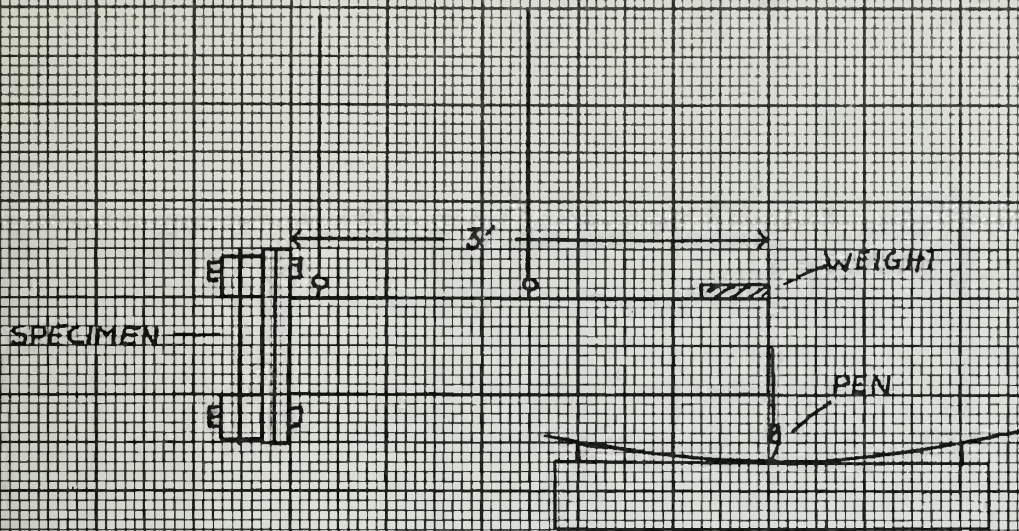


FIG. 1 BALLISTIC PENDULUM

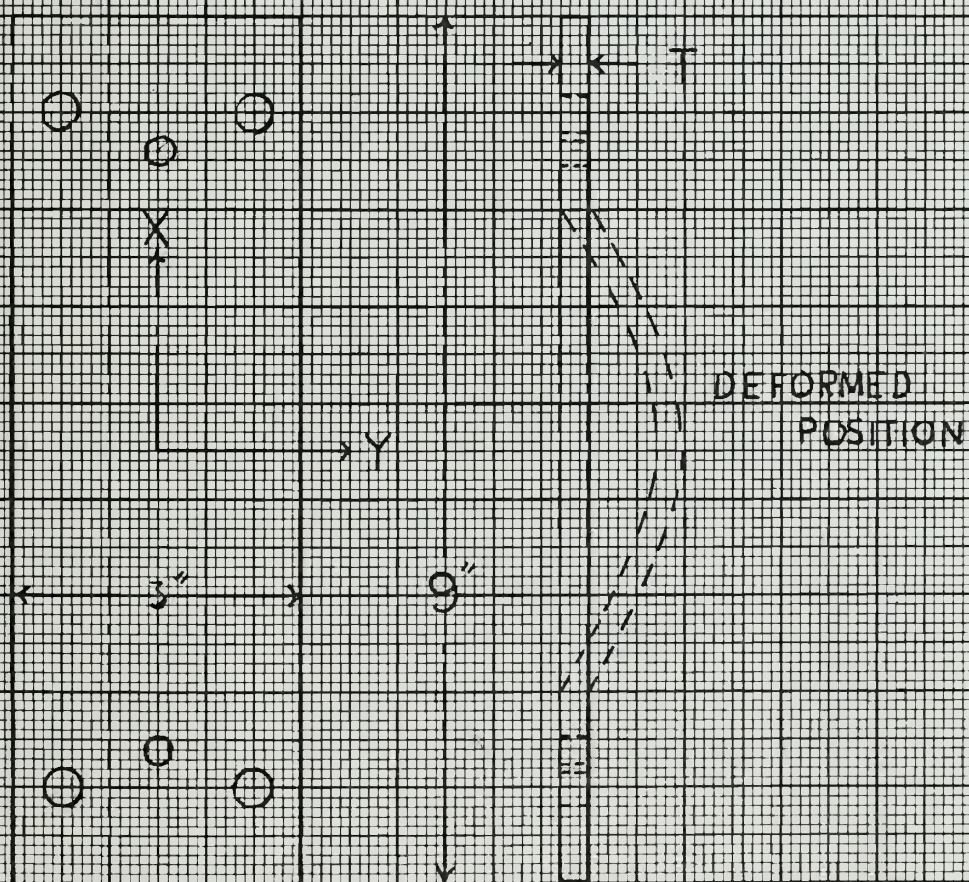
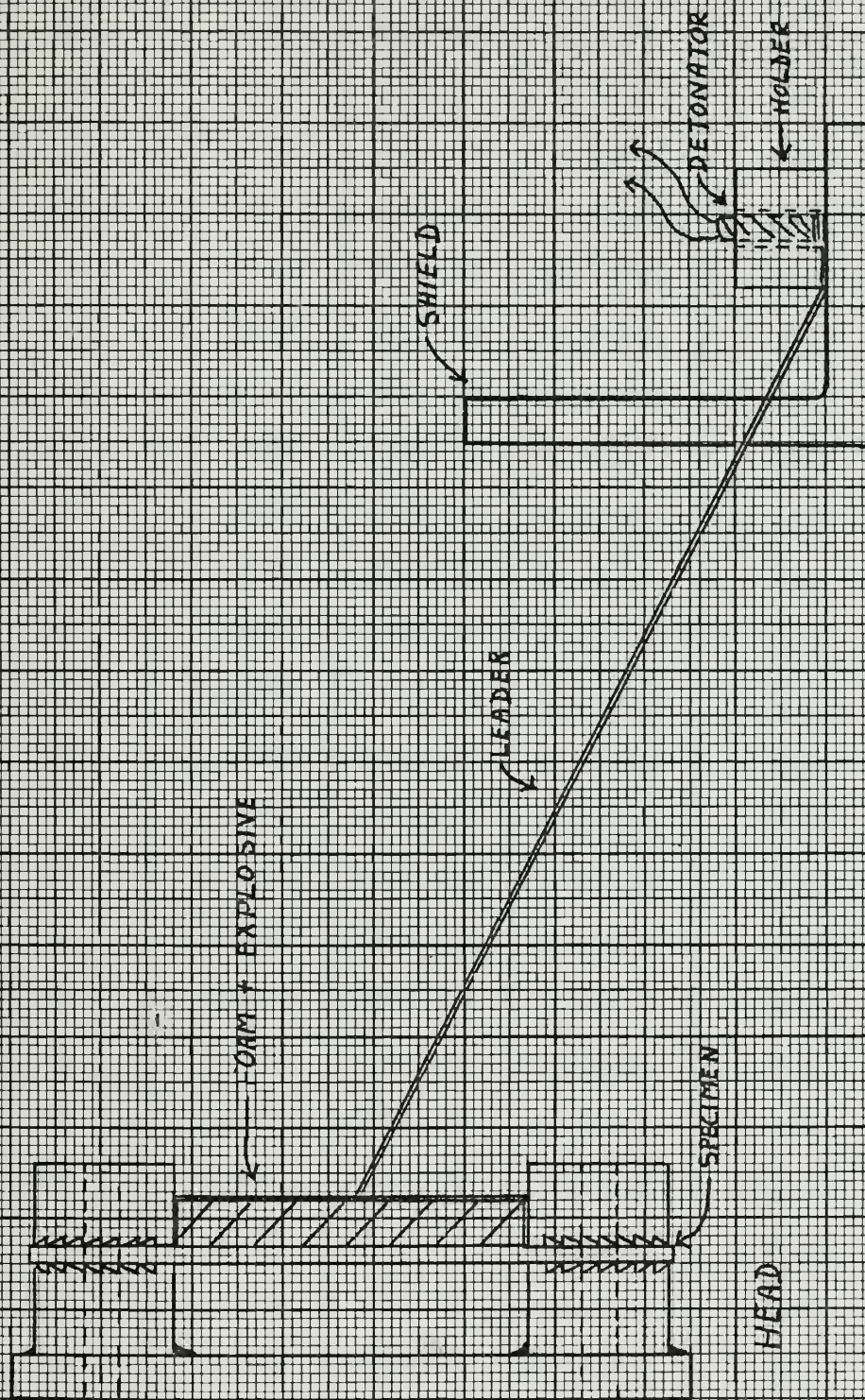


FIGURE 2 SPECIMEN



HEAD + EXPLOSIVE ARRANGEMENT

FIGURE 3

TABLE 1

Specimen No.	Thickness (in)	Vo (in/sec)	Plate Wt. (lbs)	Wmax (in)	Wc (in)
1	.1728	--	0.72371	.28	.268
2	.1729	1326.74	0.72437	.386	.354
3	.1729	1215.36	0.72413	.267	.246
4	.1729	1744.80	0.72388	.382	.356
5	.1728	2110.08	0.72371	.601	.549
6	.1727	1849.53	0.72305	.377	.363
7	.0988	2592.74	0.41685	.578	.558
8	.0988	1574.09	0.41351	.385	.342
9	.0988	2952.95	0.41337	.83	.775
10	.0987	1788.40	0.41656	.403	.362
11	.0988	1348.73	0.41712	.3025	.283
12	.0987	2068.51	0.41670	.550	.491
14	.0642	2679.50	0.26824	.6825	.6825
15	.0644	1936.77	0.26926	.480	.480
16	.0646	2460.96	0.26973	.6385	.631
19	.0642	1805.96	0.26824	.451	.409
20	.0643	3142.00	0.26884	.825	.825
23	.1752	1054.26	0.48326	.178	.178
25	.0744	1621.06	0.31348	.3625	.3435
26	.1780	1641.04	0.74974	.3155	.296
27	.1770	894.90	0.25507	.1035	.1035
28	.1766	2028.78	0.74261	.433	.412
29	.1781	771.95	1.2532	.112	.105
30	.1768	1427.99	0.49712	.278	.267
31	.1778	1267.03	0.26398	.248	.248
33	.1760	1080.72	1.24734	.1985	.192

TABLE 1 (Cont.)

#	Wc/t	Half Swing (in)	End Angle (min)	Explosive Amt. (mil)	Leader Type	Attenuator Type
1	1.54	--	34	15	Center	Foam
2	2.05	7.525	17	15	Side	Neo.
3	1.42	6.42	34	15	Center	Neo.
4	2.06	9.03	31	20	Center	Foam
5	3.18	12.45	34	30	Side	Neo.
6	2.10	9.575	31	30	Center	Foam
7	5.65	8.14	4	20	Center	Foam
8	3.46	4.84	7	10	Tri.	Neo.
9	7.85	9.1	0	20	Tri.	Neo.
10	3.67	5.55	7	15	Center	Foam
11	2.87	4.19	4	10	Center	Foam
12	4.98	6.81	4	15	Side	Neo.
14	10.65	5.375	-10	15	Center	Foam
15	7.46	3.9	-10	10	Center	Foam
16	9.77	4.96	-7	10	Tri.	Neo.
19	6.37	3.625	-24	10	Center	Foam
20	12.82	6.325	-14	15	Tri.	Neo.
23	1.015	4.13	34	15	Center	Foam
25	4.62	3.8	0	10	Center	Foam
26	1.66	8.625	31	25	Center	Foam
27	.585	1.85	38	15	Center	Foam
28	2.33	10.55	24	30	Center	Foam
29	.59	7.05	31	10	Center	Foam
30	1.51	5.75	31	20	Center	Foam
31	1.395	2.72	31	20	Center	Foam
33	1.09	9.825	28	15	Center	Foam

TABLE 1 (Cont.)

#	Remarks	λ	Total Pendulum Wt. (lbs)	Specimen Width (in)	α
1	No Track	--	81.2	2.976	--
2	1	29.4	76.5	2.977	1.1227
3		24.67	81.2	2.976	1.1032
4		50.86	83.8	2.975	1.1859
5	1	74.46	73.2	2.976	1.2317
6	3	57.27	83.8	2.975	1.1996
7	1,3	374.44	80.6	2.998	1.1478
8		138.01	80.6	2.974	1.0387
9	1	485.71	80.6	2.973	1.1780
10		178.51	80.6	2.999	1.0654
11		101.32	80.6	3.000	1.0071
12	3	238.81	75.9	3.000	1.0968
14	3	891.47	80.4	2.969	1.0599
15	2	436.00	80.4	2.971	0.9939
16	1	742.92	80.4	2.967	1.0433
19	1	405.09	80.4	2.969	0.9793
20	1,3	1222.34	80.4	2.971	1.0946
23		18.08	73.8	1.960	1.0751
25		257.37	80.4	2.994	0.9872
26		42.45	85.8	2.993	1.1783
27		12.77	74.0	1.024	1.0426
28	3	65.91	85.8	2.988	1.2274
29		9.83	82.1	5.000	1.0134
30		32.58	73.9	1.998	1.1444
31		25.36	73.8	1.055	1.1886
33		18.83	82.1	5.036	1.0814

TABLE 1 ADDENDUM

- (1) Specimen number refers to the identification marked on each specimen as it was cut. The original location of each specimen is plotted in Figures 26 through 28.
- (2) Plate weight is a measure of the mass of only that portion of the specimen that was subject to loading (i.e., the part not in the clamps was not included).
- (3) Deflection: W_{max} is the maximum deflection of the plate.
 W_c is the maximum deflection along the longitudinal center-line.
- (4) End Angle is a measure of the rotation of the clamped ends of the specimen after being released from the head (in the same direction as the deflection is plus; away, minus).
- (5) Remarks Code:
 1. The specimen slipped slightly in the clamps.
 2. The detasheet used was perforated.
 3. The deflections of the specimen are graphed in figures 8 through 19.
- (6) λ is a non-dimensional impulse parameter (see Figure 7).
- (7) $\alpha = \left(\frac{2 V_0 t}{D L^2} \right)^{1/p}$ (Figure 7)
- (8) The length of all specimens was 5.046 inches.

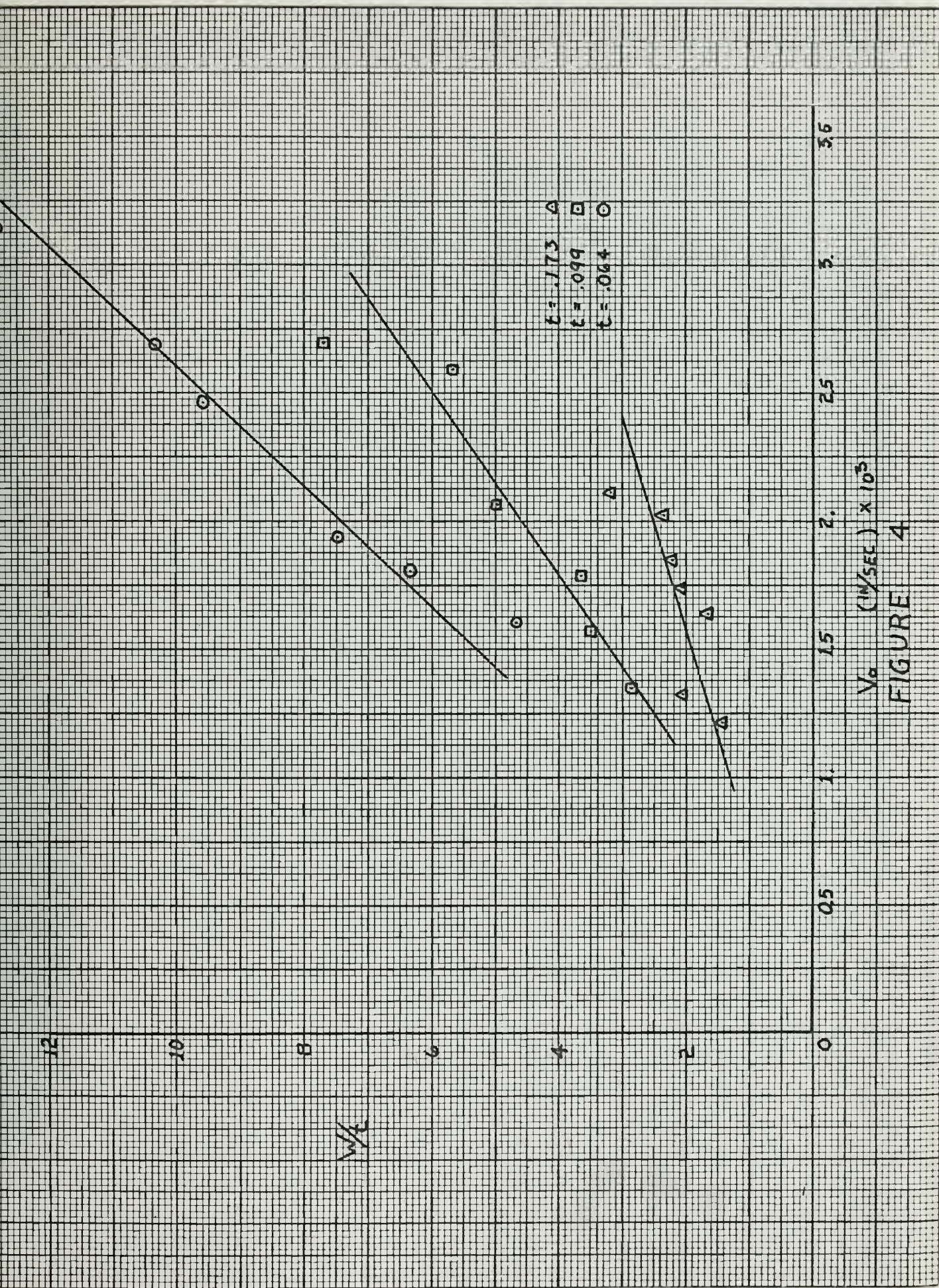
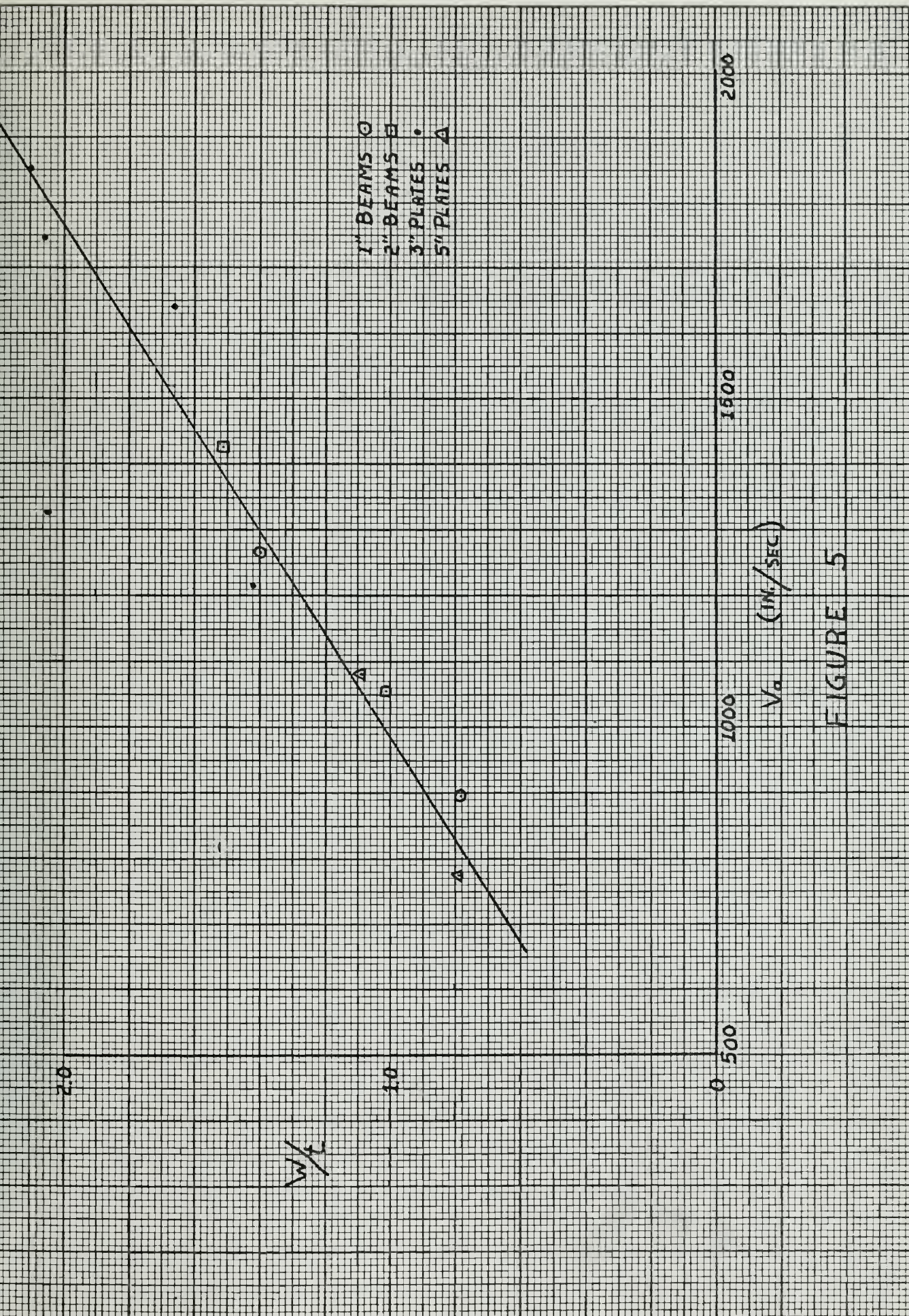


FIGURE 4

FIGURE 5



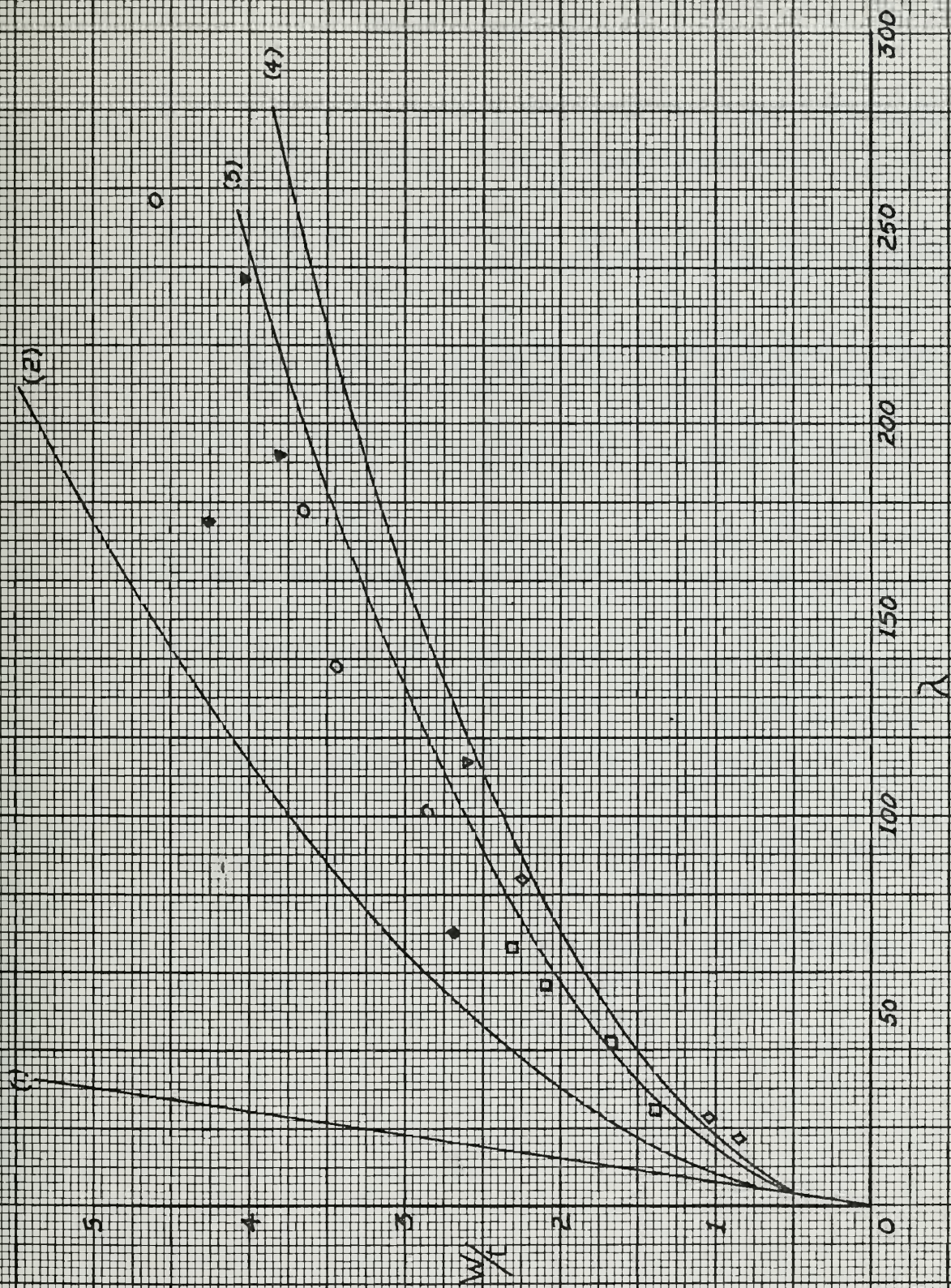


FIGURE 6

FIGURE 7

Legend for Figure 6

The curves in figure 7 were plotted from reference [7.]

- (1) Simple Bending Theory, Rigid-Perfectly Plastic Material
- (2) Lower Bound Prediction of Jones [7] for a beam with clamped supports and made from a rigid, perfectly plastic material
- (3) Lower Bound Prediction of Jones [7] for a beam with clamped supports and made from a rigid, strain rate sensitive material with $\alpha = 1.1487$
- (4) Upper Bound Prediction for the same conditions as (3)

◇ Jones results	$L/t = 31.7$	$\sigma_0 = 30,466$ psi
◇ Humphreys results	$L/t = 47.7$	$\sigma_0 = 26,800$ psi
⊙ 3" Plate results	$L/t = 51.1$	$\sigma_0 = 33,800$ psi
□ 3" Plate results	$L/t = 28.8$	$\sigma_0 = 36,800$ psi
▽ Jones results	$L/t = 45.75$	$\sigma_0 = 30,466$ psi

$$\lambda = \frac{\mu L^2 V_0^2}{\frac{\sigma_0 t^3}{4}}$$

$$\alpha = \left(\frac{2 V_0 t}{D L^2} \right)^{1/P}$$

μ = mass per unit length
 L = the half length of the specimen
 V_0 = initial velocity
 σ_0 = static yield stress
 t = plate thickness
 $P = 5$
 $D = 40.4$

SAMPLE # 6

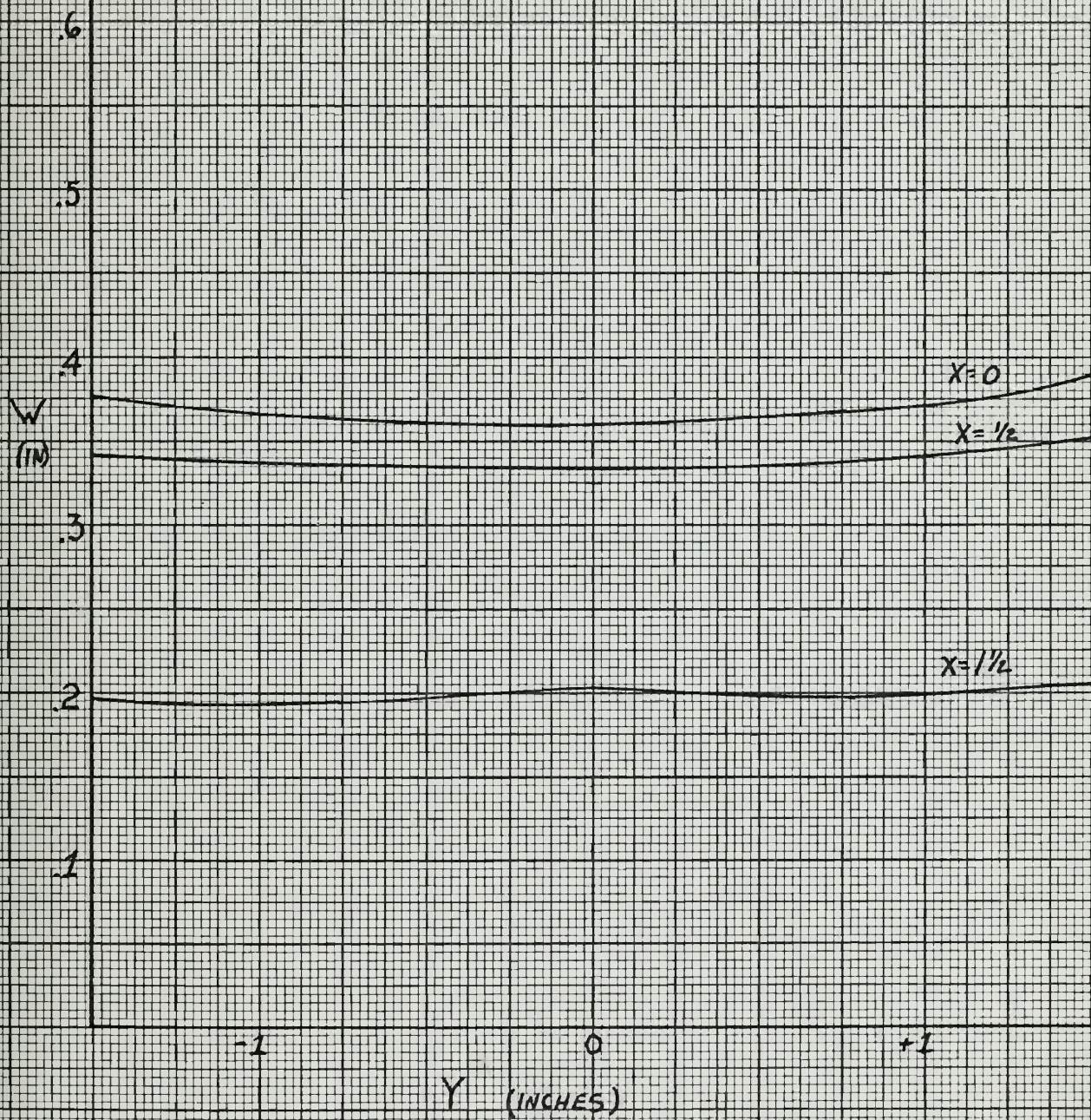


FIGURE 8

SAMPLE # 6

$\gamma = 0$ ———
* $\gamma = 1\frac{3}{8}$ - - - -

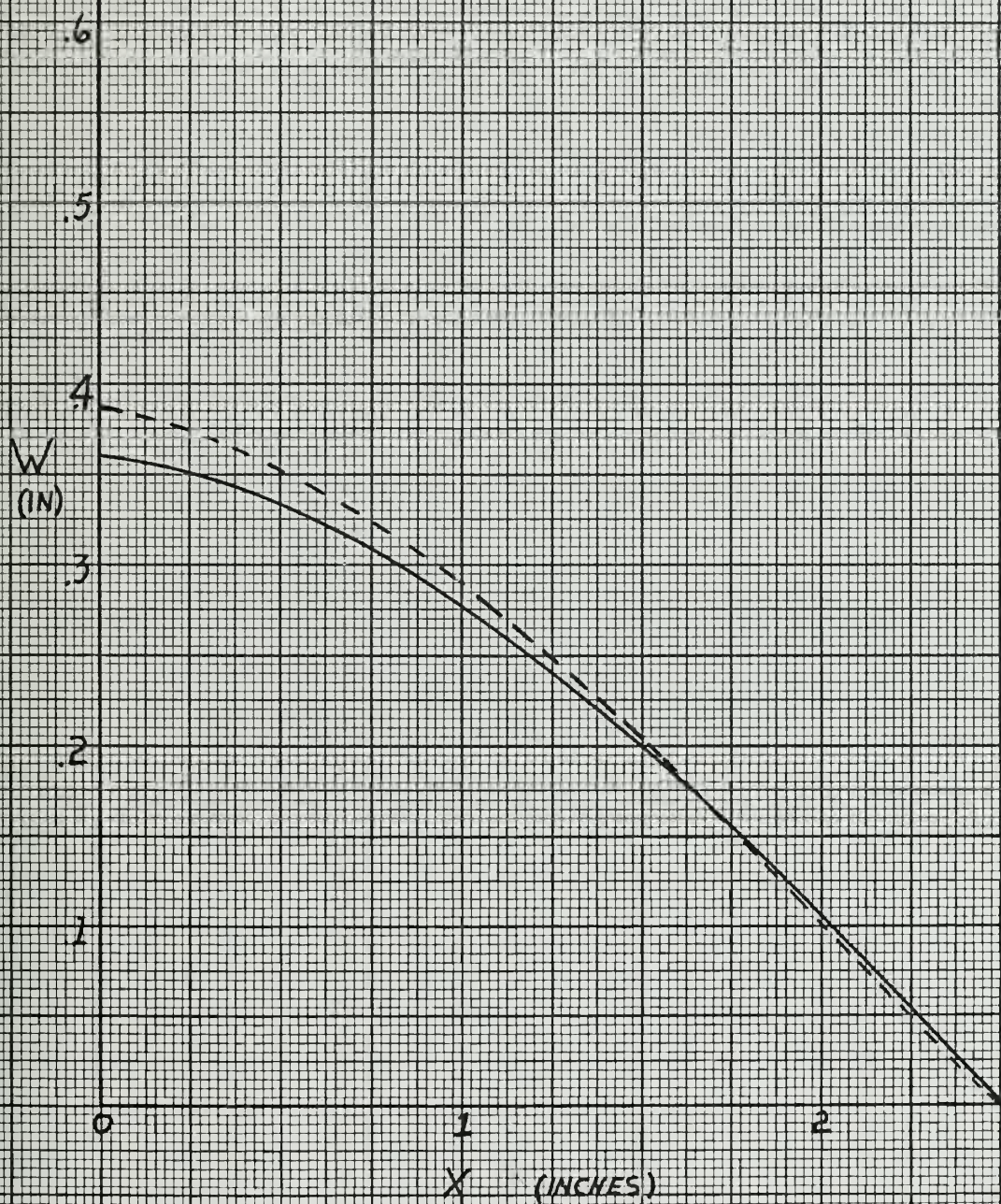


FIGURE 9

* $\gamma = 1\frac{3}{8}$ was graphed because of the curvature at the edge of the specimen.

SAMPLE # 7

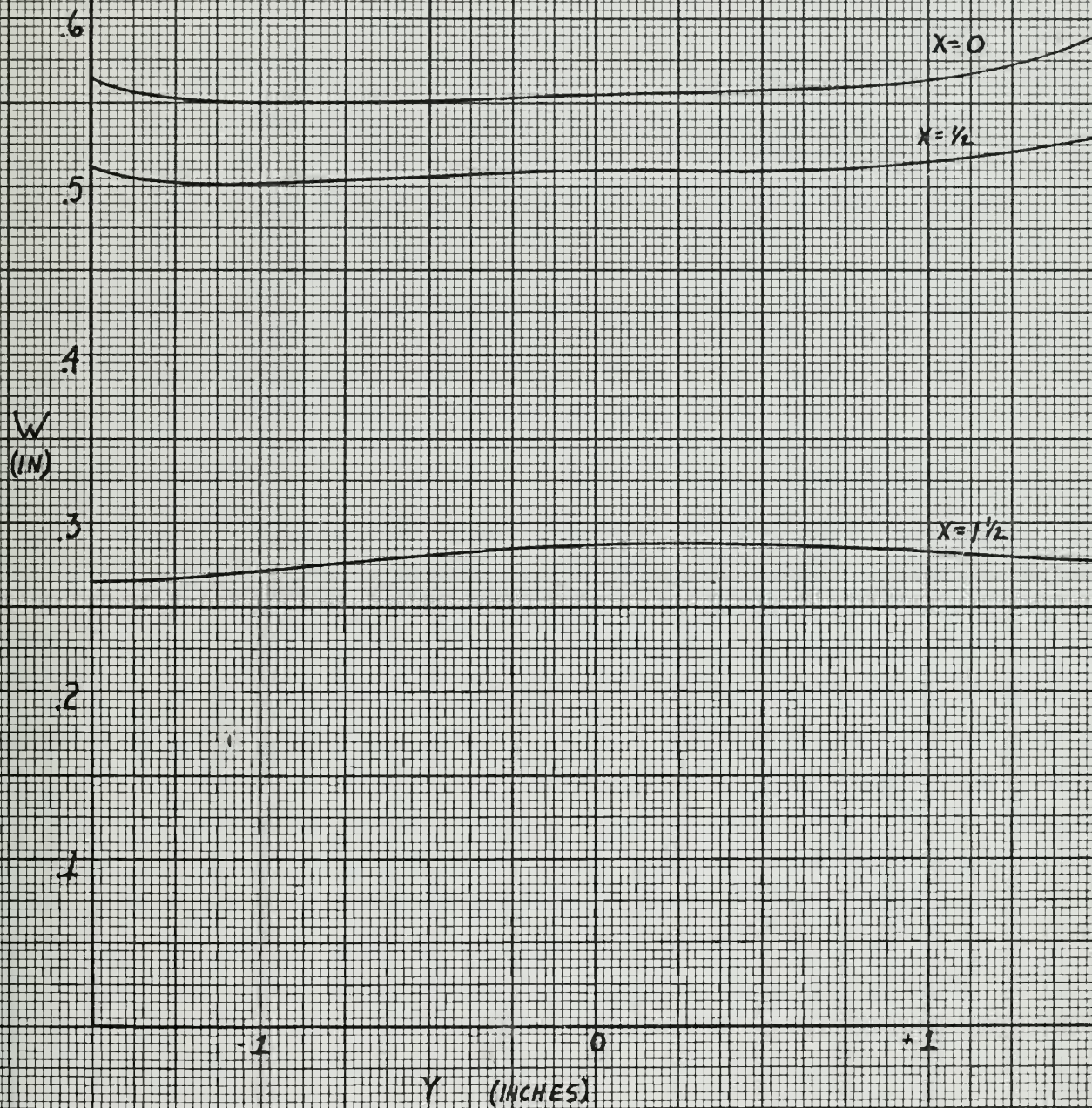


FIGURE 10

SAMPLE # 7

$Y=0$ ———

$Y=+1\frac{3}{8}$ - - - -

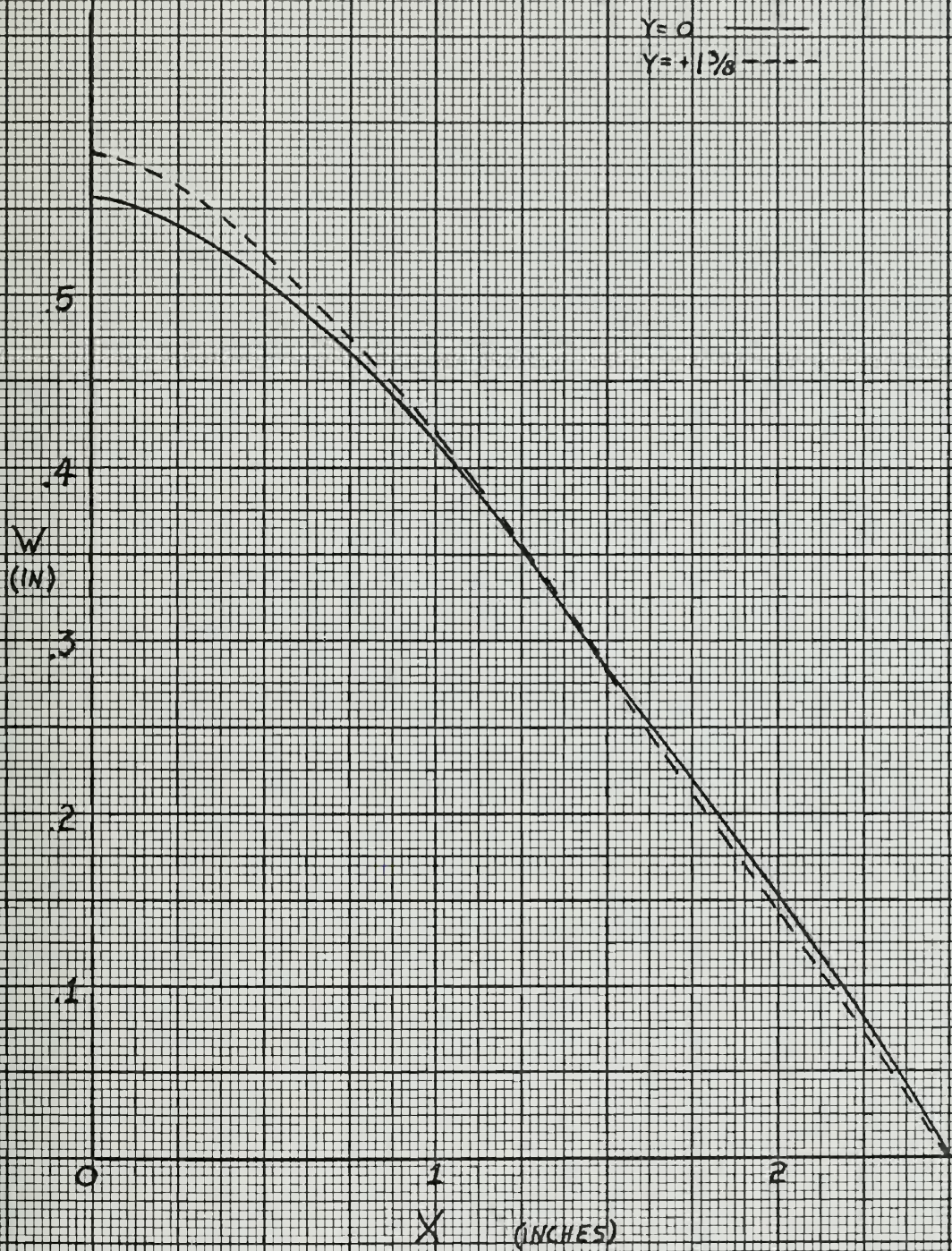


FIGURE 11

SAMPLE # 12

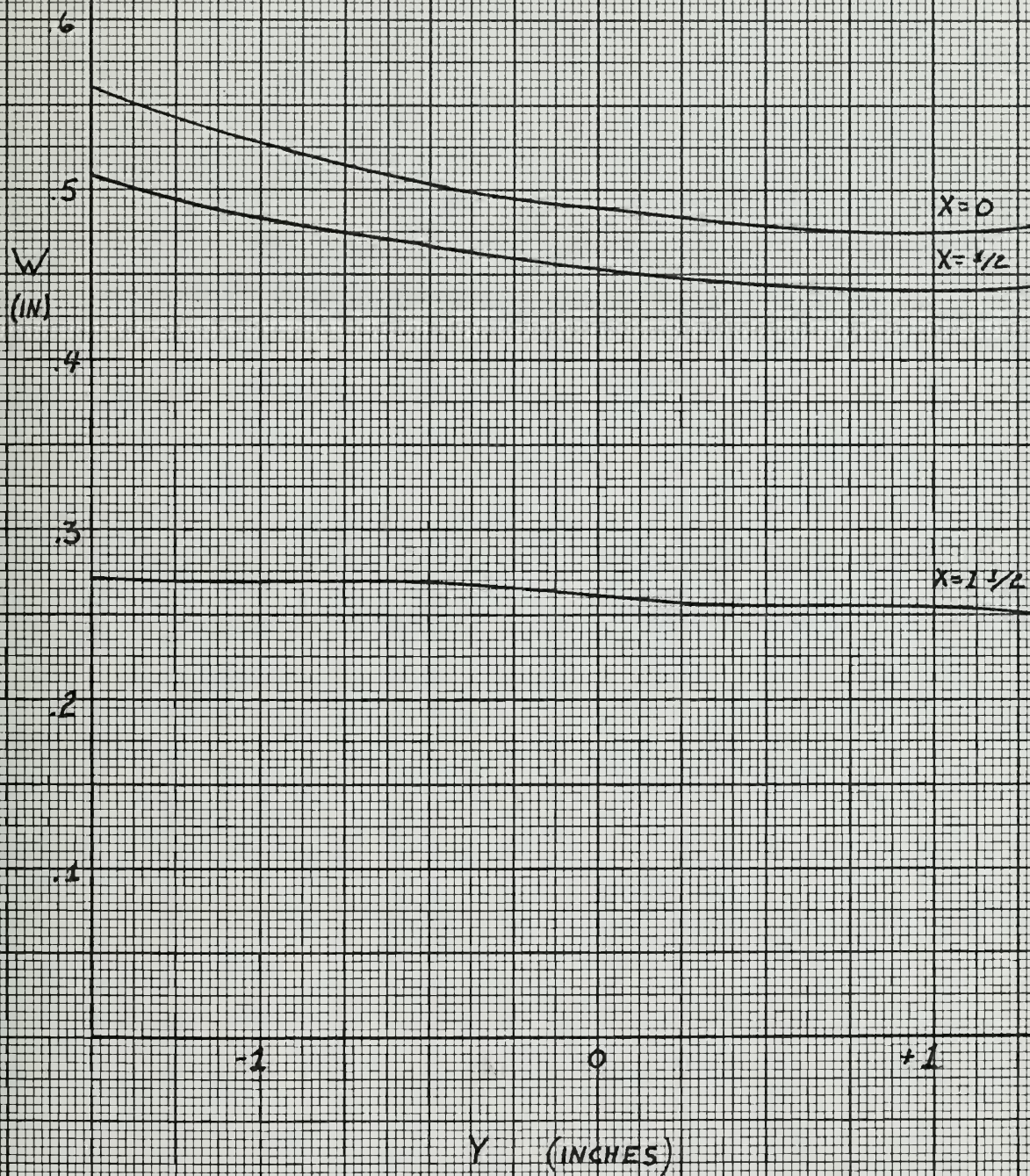
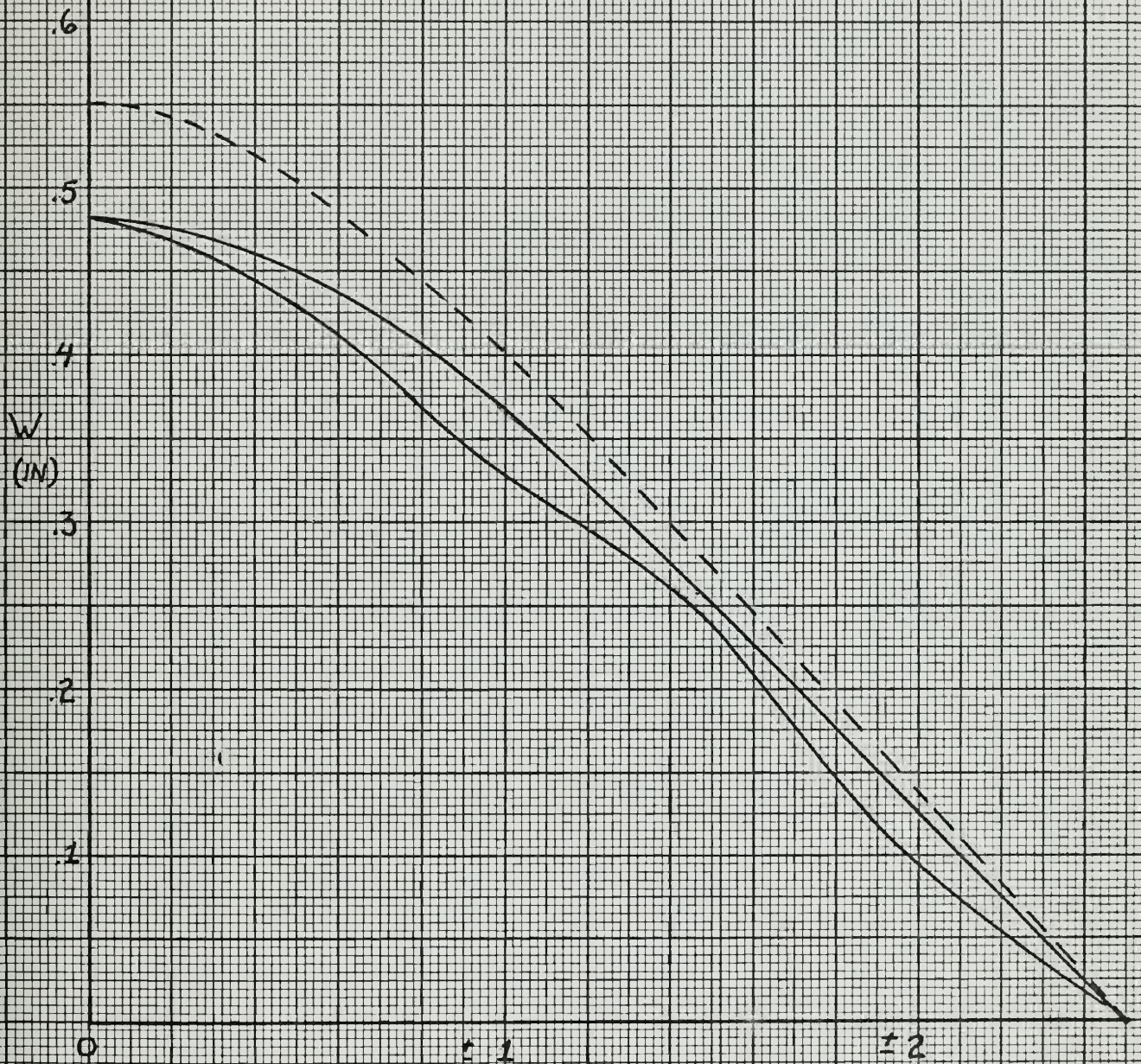


FIGURE 12

SAMPLE # 12

$y = -1/3/8$ ———

$y = +1/3/8$ - - - -



X (INCHES)
FIGURE 13.

SAMPLE # 14

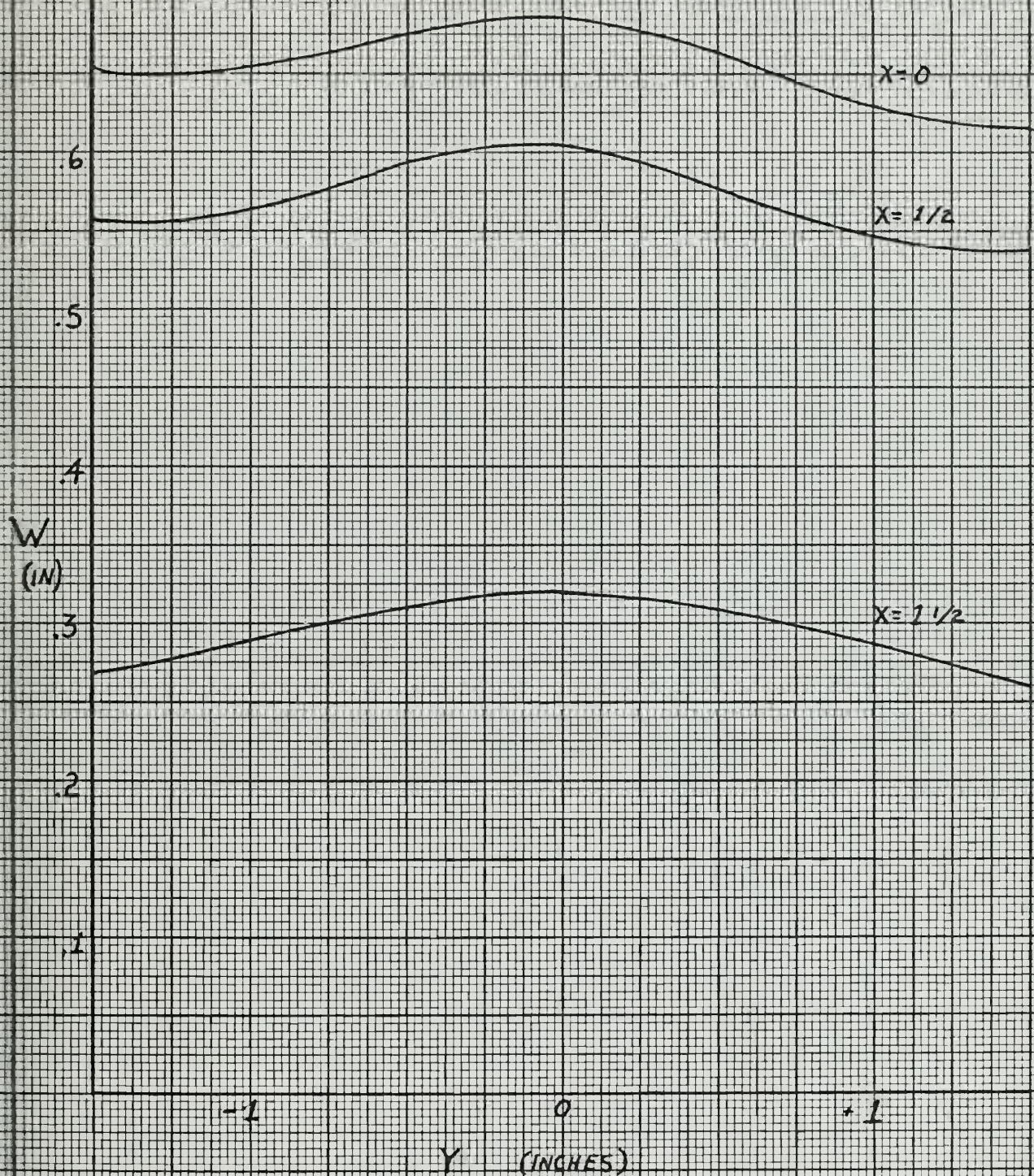


FIGURE 14

SAMPLE # 14

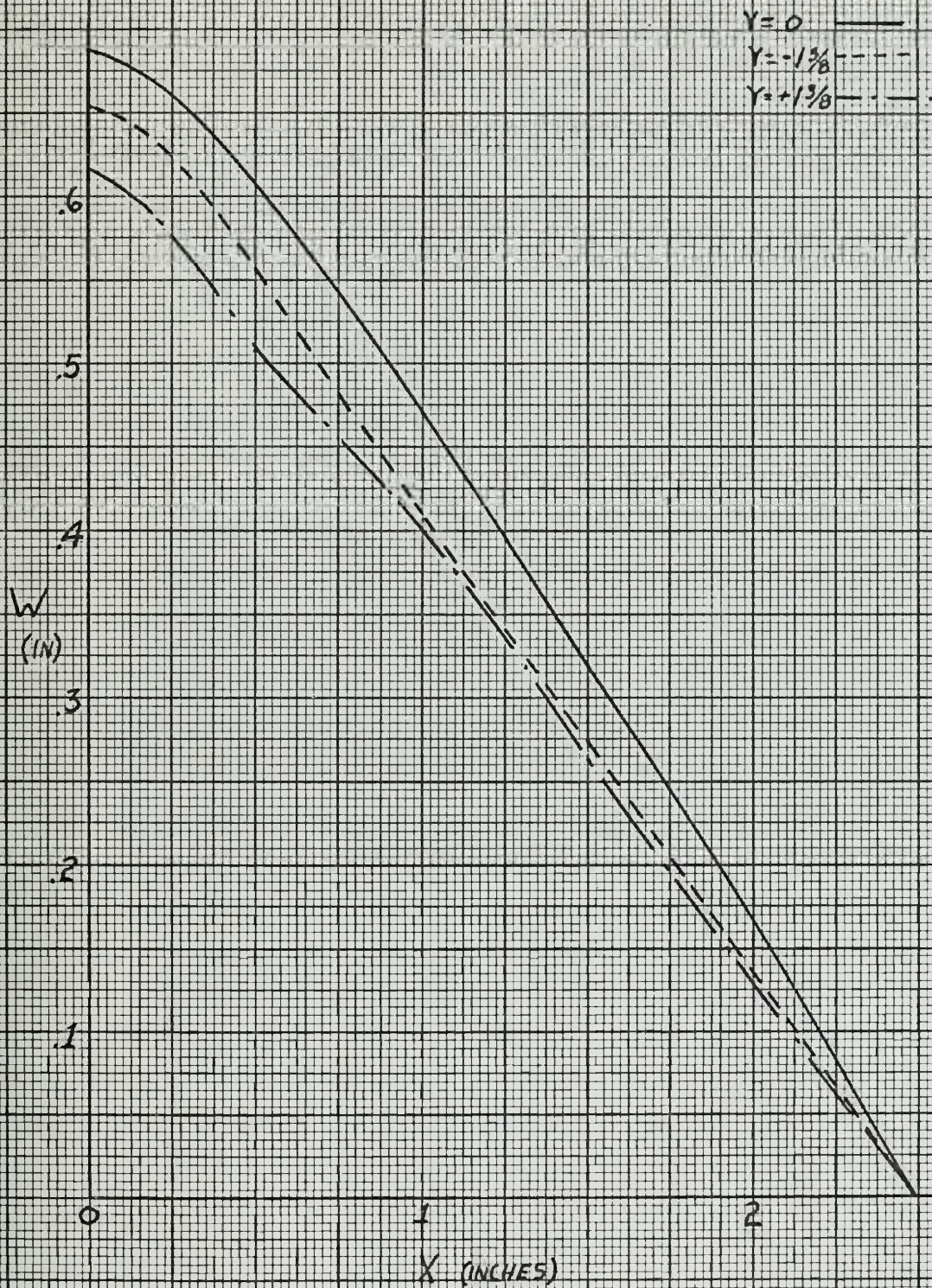


FIGURE 15

SAMPLE # 20

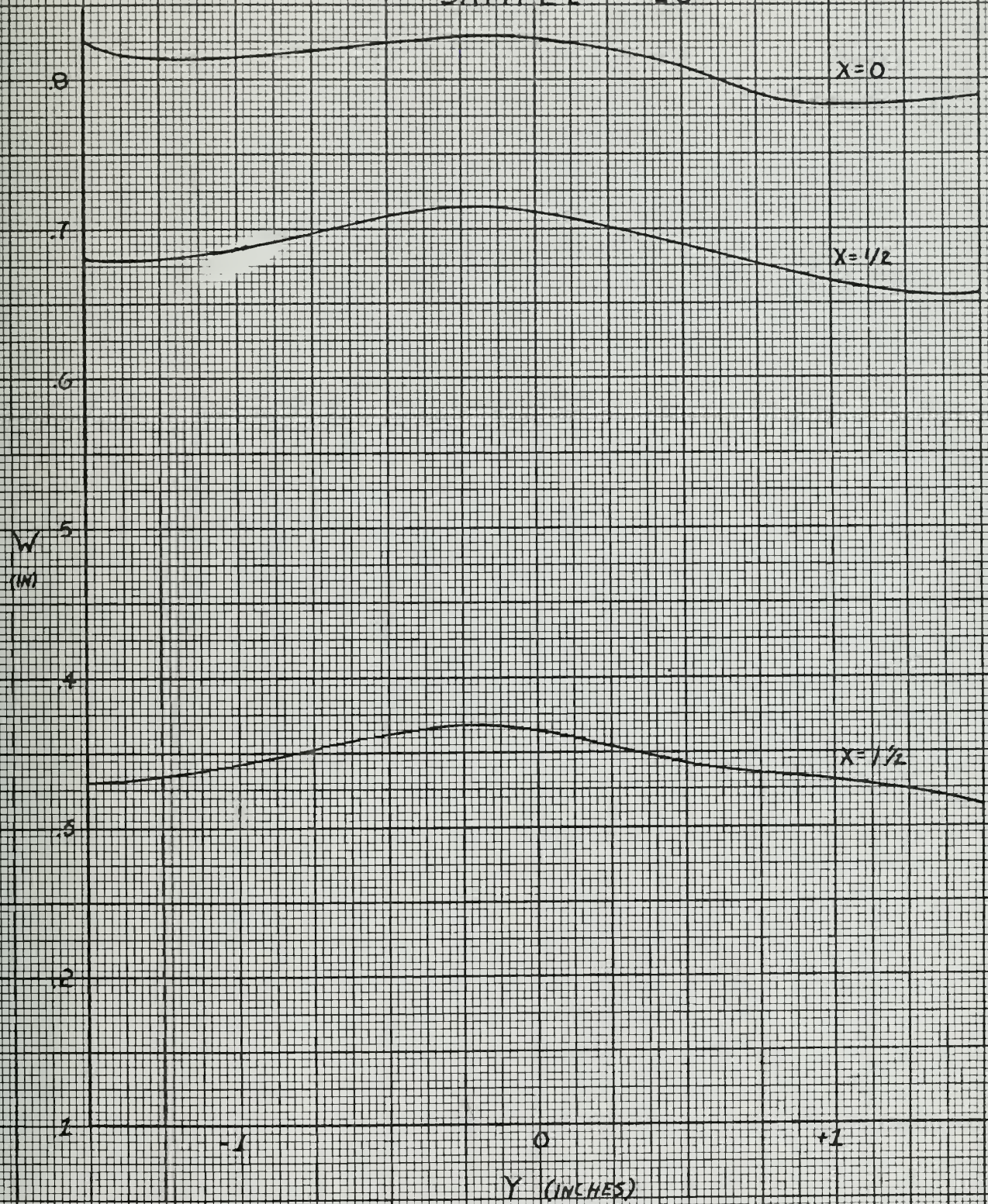


FIGURE 16

SAMPLE # 20

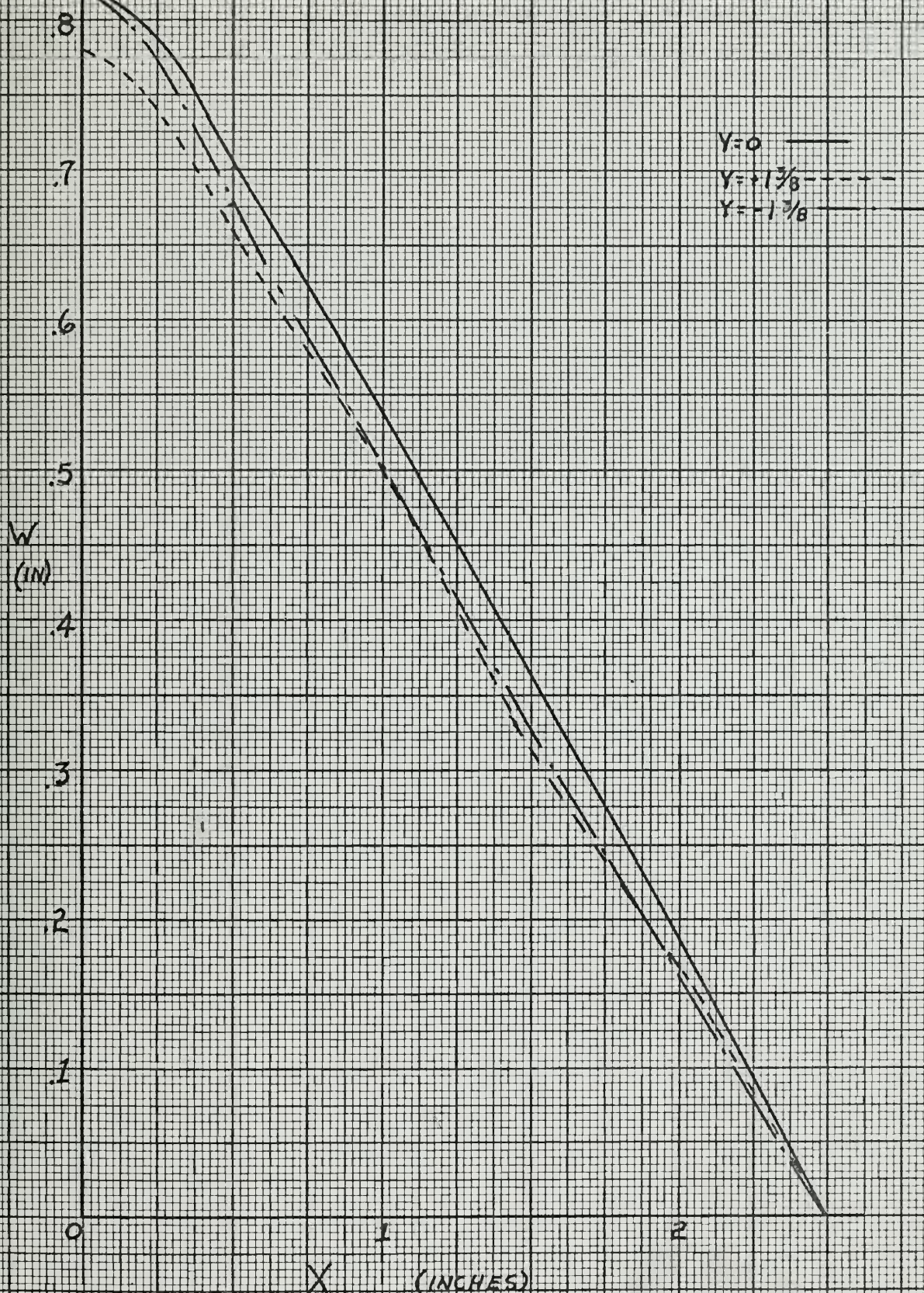
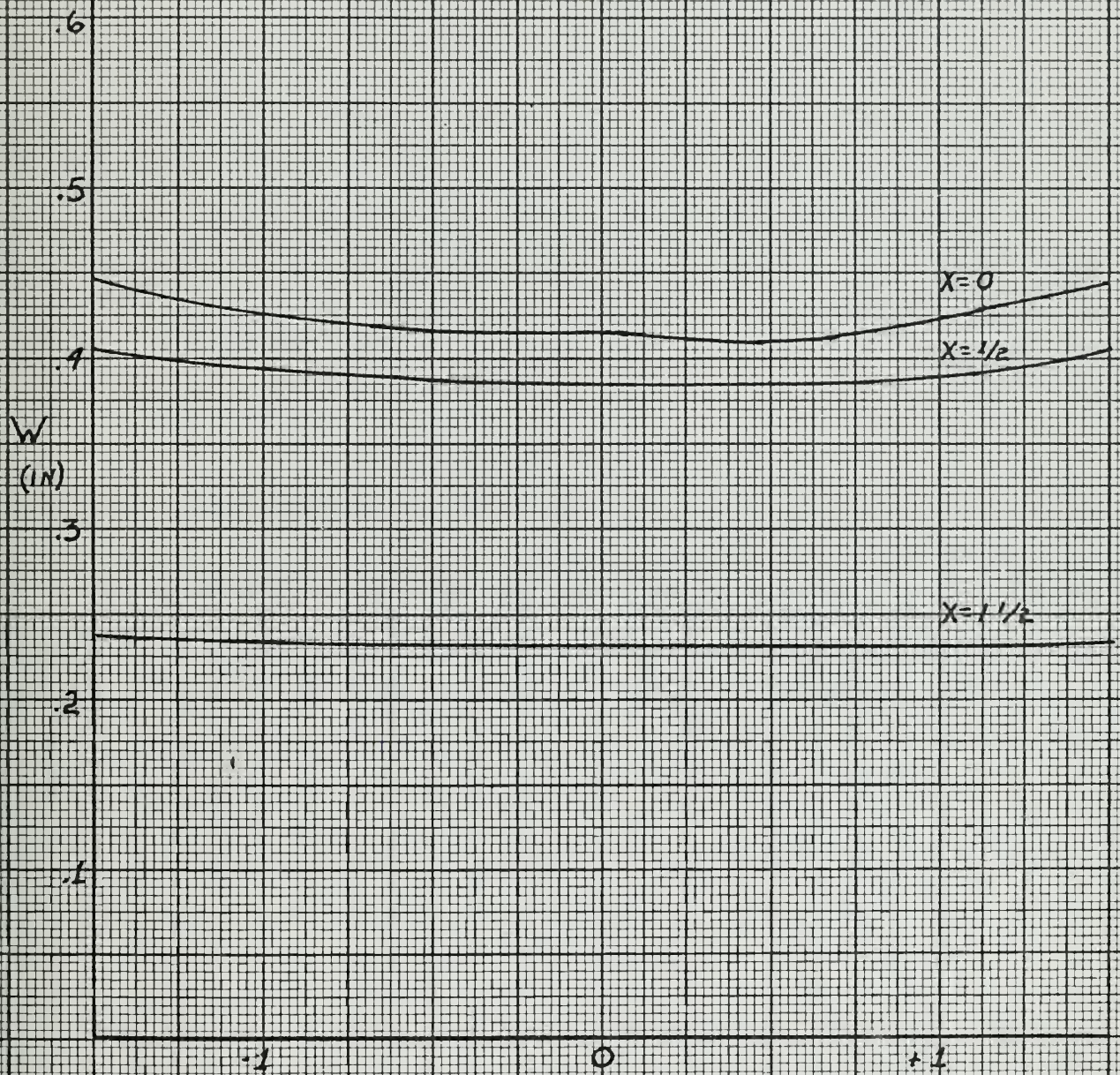


FIGURE 17

SAMPLE # 28



Y (INCHES)

FIGURE 18

SAMPLE # 28

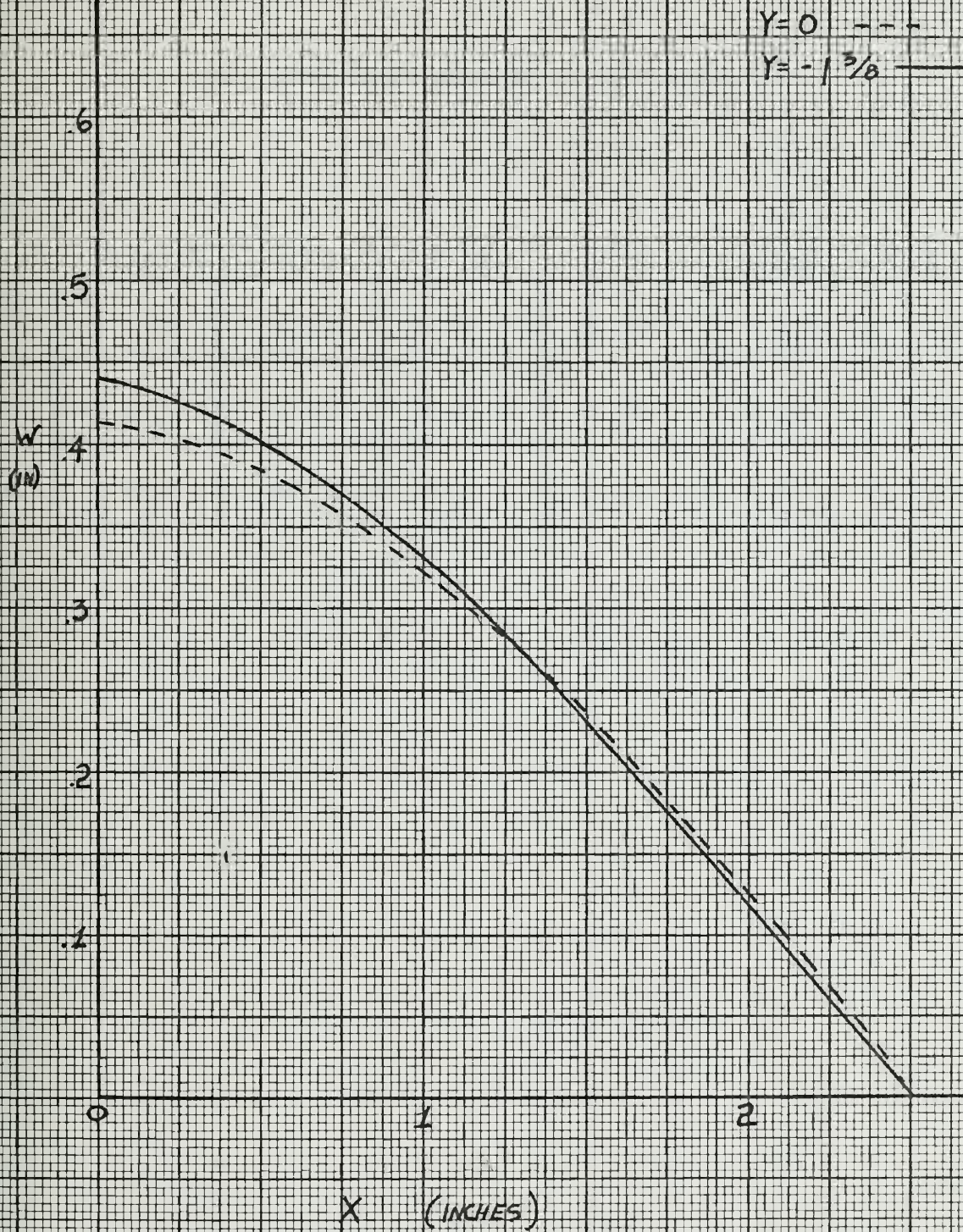


FIGURE 19

APPENDIX A

TABLE 2

Chemical Composition of Steel Plates

Plate	% C	% Mn	% P	% S	% Si
14 gage	0.071	0.41	0.008	0.021	0.001
12 gage	0.046	0.25	0.007	0.019	0.001
7 gage	0.086	0.34	0.009	0.023	0.003

APPENDIX B

#1 #2

$\sigma_y = 37,500 \text{ PSI}$
SPEED = 2 IN/MIN.

$\sigma_y = 36,100 \text{ PSI}$
SPEED = .05 IN/MIN.

$\sigma_{ult} = 48,000 \text{ PSI}$

2

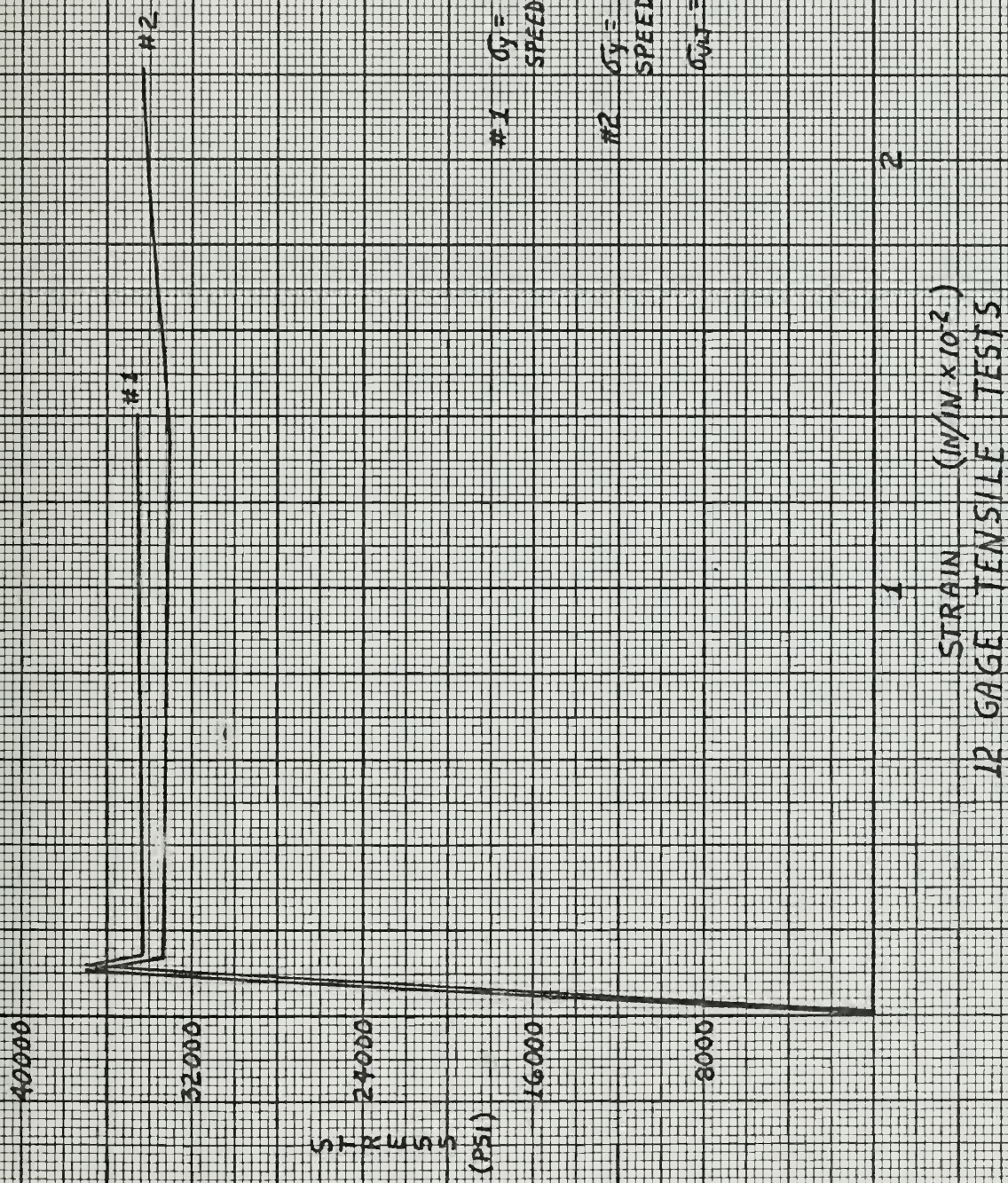
STRAIN (IN/IN) $\times 10^{-2}$

7 GAGE TENSILE TESTS

FIGURE 19A

40000
32000
24000
16000
8000

STRESS (PSI)



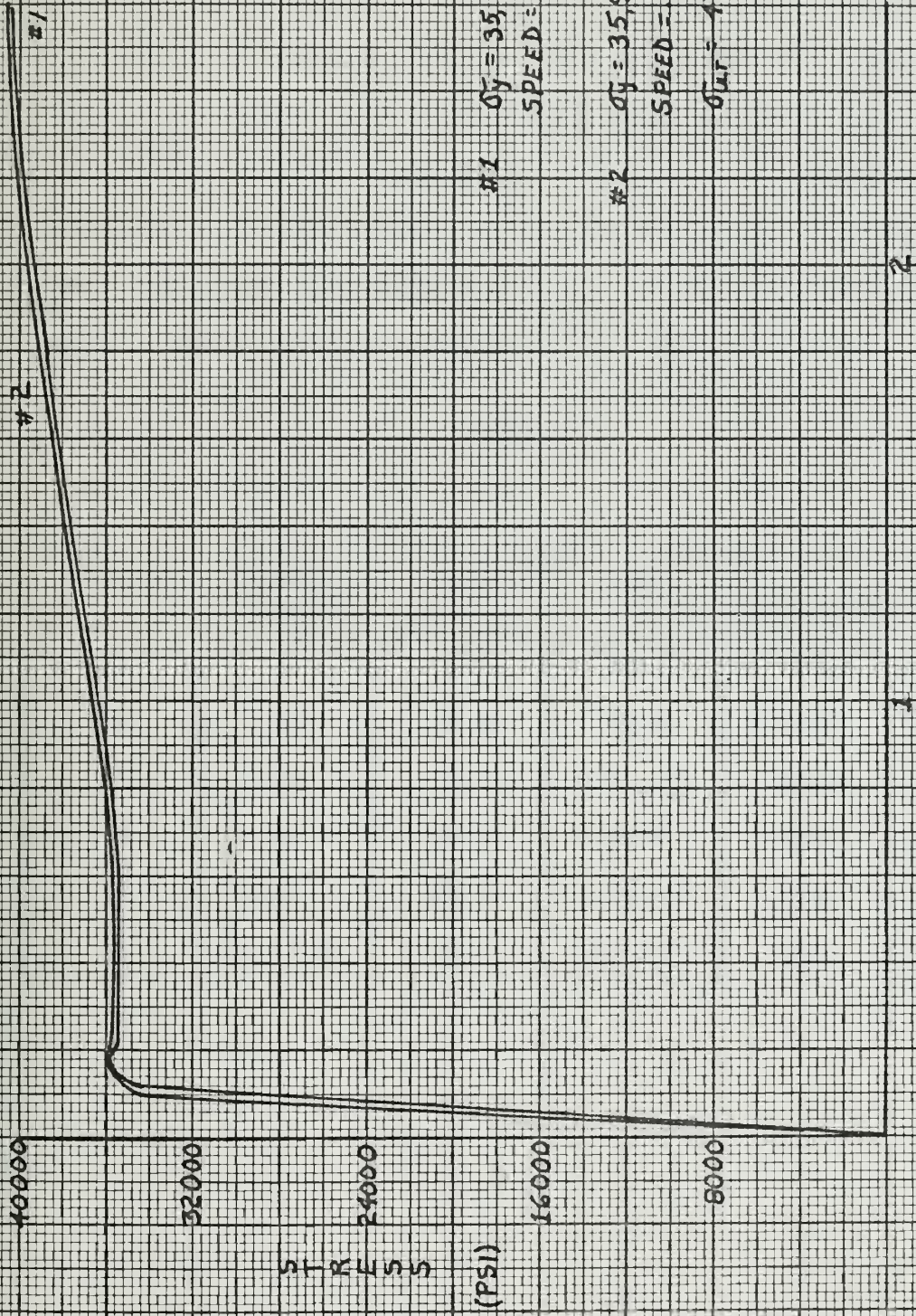
#1 $\sigma_y = 39,300$ PSI
SPEED = .2 IN/MIN.

#2 $\sigma_y = 33,300$ PSI
SPEED = .1 IN/MIN.

$\sigma_{UT} = 43,000$ PSI

12 GAGE TENSILE TESTS

FIGURE 20



14 GAGE TENSILE TESTS

FIGURE 21

APPENDIX C

The density of the steel from which the specimens were cut was determined by the water displacement method. The volume of the plate samples were calculated by observing the amount of water that they displaced in a graduated beaker. The samples were then carefully weighed and the density was calculated. It was assumed that all the steel plates had the same density; consequently, the average of all the tests was used. Table 3 is a summary of the test results.

TABLE 3

Test #	Plate (gage)	Vol. (ml)	Wt. (gms)	(gms/ltr)	Density ₃ (lbs/in ³)
1	7	9.5	72.3	7610	.275
2	12	6.9	50.8	7360	.266
3	12	4.0	31.25	7820	.283
4	14	10.0	74.8	7480	.2705
5	12-7	20.0	154.35	7720	.279
6	12-14-7	29.5	232.15	7660	.277

APPENDIX D

Windage Loss Calculation

To determine the effect of friction and other losses on the swing of the ballistic pendulum, two series of tests were performed. In the first, and previous to any experimentation, the pendulum was allowed to swing through a number of cycles. The total loss, measured on heat sensitive paper, was divided by the number of cycles to obtain an average loss. The second series was taken at the end of the experiment with measurements being made for one cycle of the pendulum at various swing amplitudes. The results of the tests are in Table 4. Figure 23 is a plot of loss versus amplitude.

It is noteworthy that the losses are small --- the range being 0.6 percent to 1.6 percent of the half swing. In addition, they may be considered an upper bound as the loss of only one quarter of a cycle would be used to correct the plate test data. Since the heat sensitive paper can only be read to an accuracy of one tenth of a centimeter, no corrections were used.

TABLE 4

Windage Loss Results

Half Swing (cm)		Cycles	Loss/Cycle (cm)	% Loss
Max	Min			
5.9	3.6	50	.05	0.95
6.95	6.6	4	.0875	1.3
3.25	3.05	4	.05	1.6
6.15	5.85	5	.06	1.0
9.0	8.7	5	.06	0.68
9.8	9.5	5	.06	0.62
4.9	4.75	5	.03	0.62
10.0	9.95	1	.05	0.5
11.25	11.2	1	.05	0.45
13.55	13.45	1	.1	0.74
14.75	14.675	1	.075	0.51
25.9	25.85	1	.05	0.31
18.45	18.35	1	.1	0.54
18.7	18.55	1	.15	0.74
20.4	20.275	1	.125	0.61
21.1	21.0	1	.1	0.47

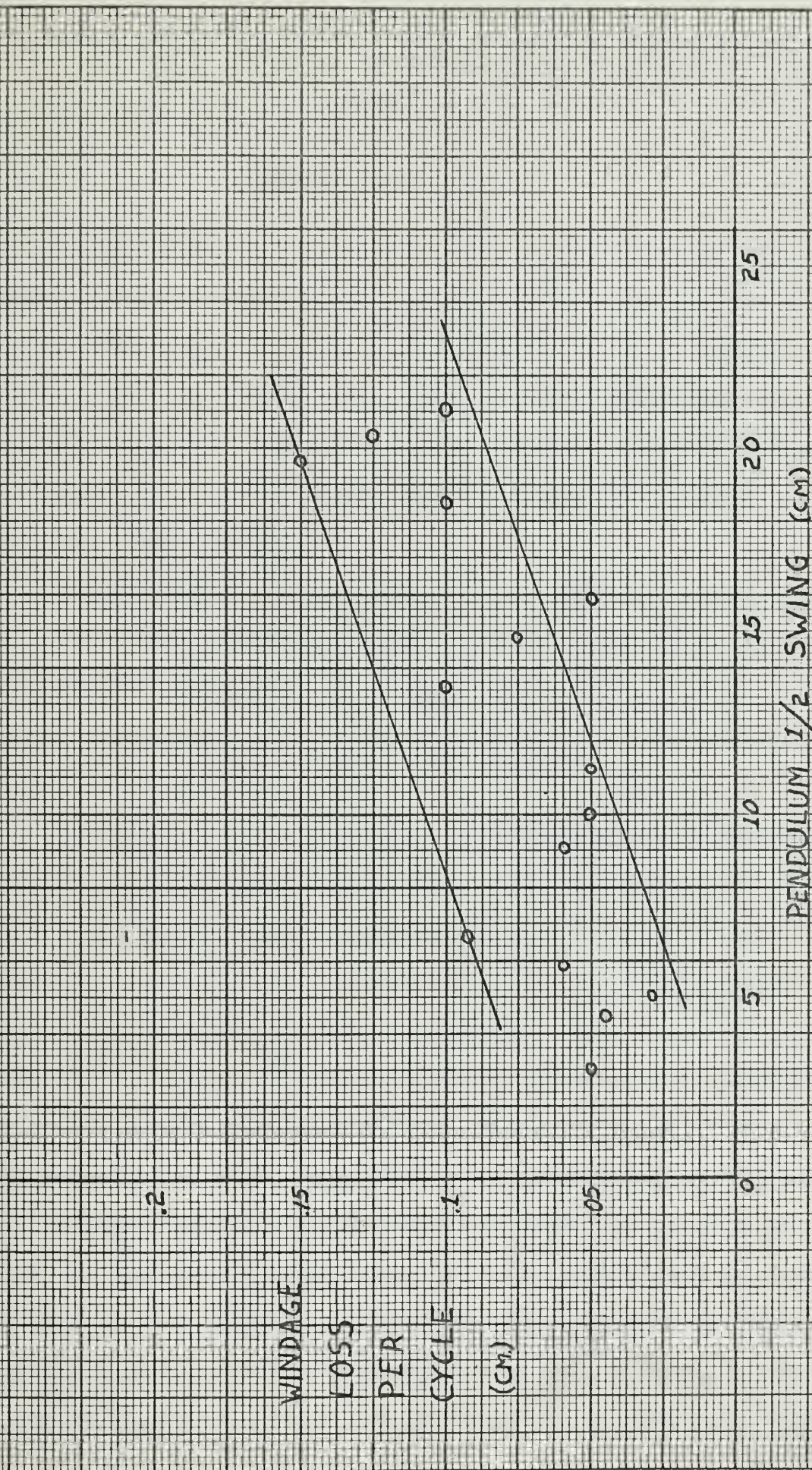


FIGURE 22

APPENDIX E

Strain Gage Results

To provide some information on strain rate and strain history of the specimens, six strain gages were placed at the centers of several plates. These gages consisted of four B.L.H., SR-4, Type PA-3 wire gages and two Budd Metalfilm Type HE-111 gages. Both types are designed for high elongation dynamic use. The gages were attached with B.L.H., SR-4 Post Yield cement.

On the whole, the results of the tests were disappointing. The first failure occurred when the gage leads broke at the soldered connection as a result of inertia forces. This problem was corrected by securing the leads to the back of the plates with electrical tape.

A second problem developed in triggering the oscilloscope fitted with a polaroid camera which was used to record the gage reading. The detonator firing voltage could not be used because there was approximately a forty microsecond delay between the firing signal and the plate deflection. To actuate the oscilloscope at the proper time a fine wire connected to a battery and the oscilloscope was taped to the explosive leader. The explosion severed the wire, triggering the camera and oscilloscope.

Another problem encountered was that the blast wave would cut the strain gage leads if they were placed too near the edge of the specimen. Shielded wire was used to overcome this difficulty. It was also found helpful to tape the wire

to the head away from the blast wave.

Table 5 summarizes the above test results.

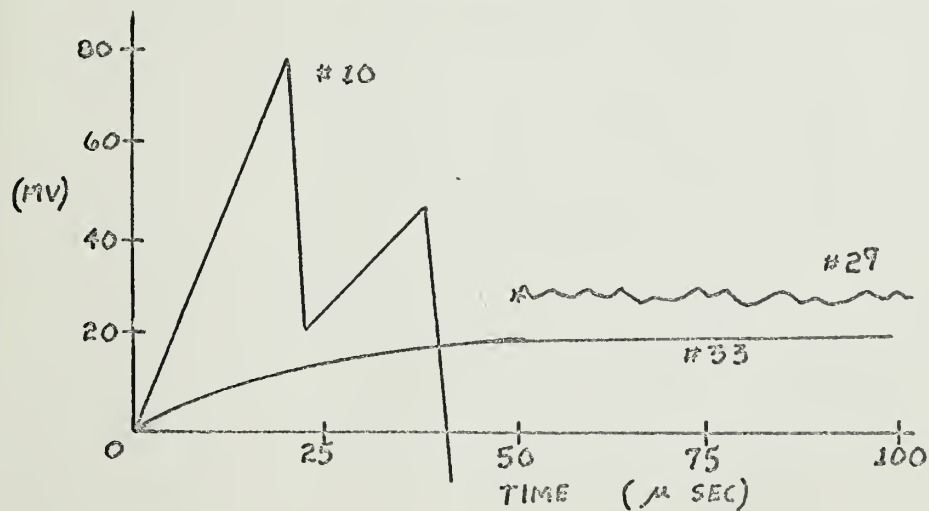
TABLE 5
Calibration

R cal (Ω)	Scope Reading (mv)	ϵ (in/in)
4500	20	.0134
2300	40	.0268
1760	60	.0350
1330	80	.0463

Test Results

Gage Type	Specimen #	W (in)	ϵ_{\max}	$\dot{\epsilon}$ (1/sec)	Remarks
PA-3	19	.409	--	--	Leads Broken
PA-3	4	.356	--	--	Leads Broken
PA-3	10	.362	.04630	2315	Leads Broken
PA-3	26	.296	--	--	Weld Failure
Budd	29	.105	.01875	--	Poor Picture
Budd	33	.191	.02310	495	

OSCILLOSCOPE PICTURE

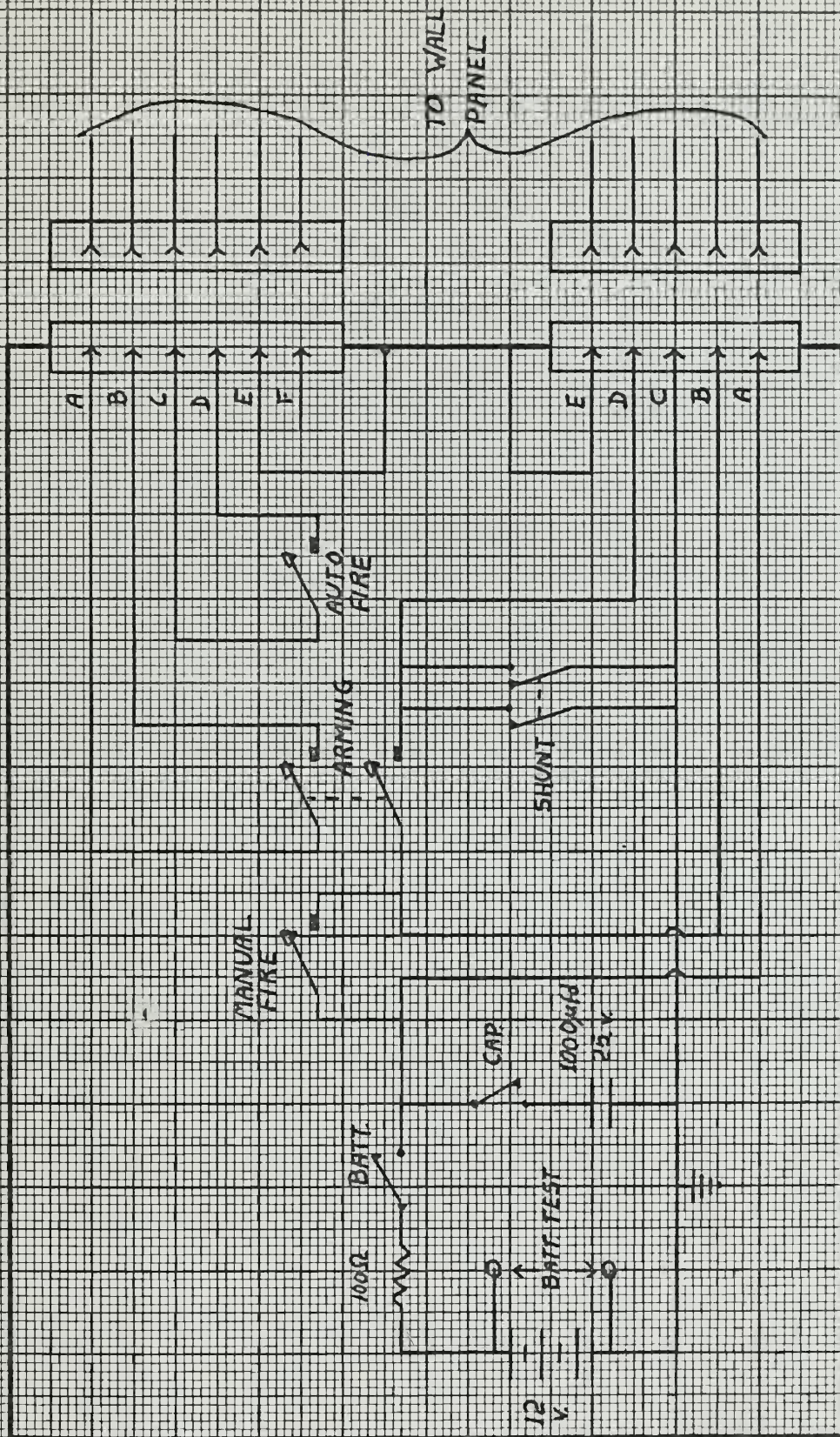


APPENDIX F

Test Chamber Firing Circuit

A detailed schematic of the firing circuit is presented in three parts. Figure 24 is the portable remote panel which is connected by two cables to a panel on the blast chamber wall (Figure 25). Also connected to the wall panel is the chamber door interlock and warning circuit (Figure 26).

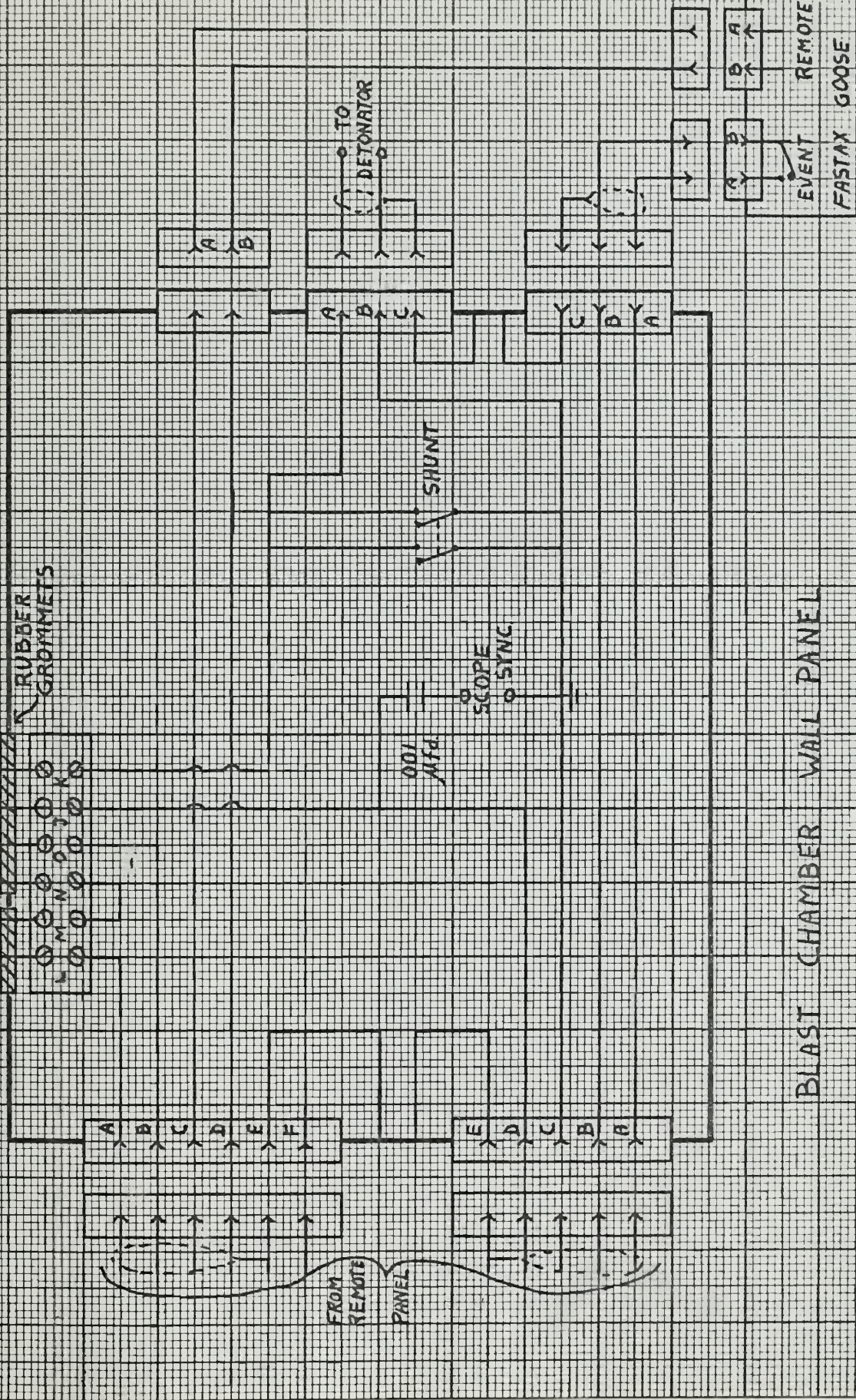
Much of the credit for this circuit is due Mr. Fred Merlis who turned a rough sketch into the working hardware and detailed drawings.



REMOTE FIRING PANEL
FIGURE 25

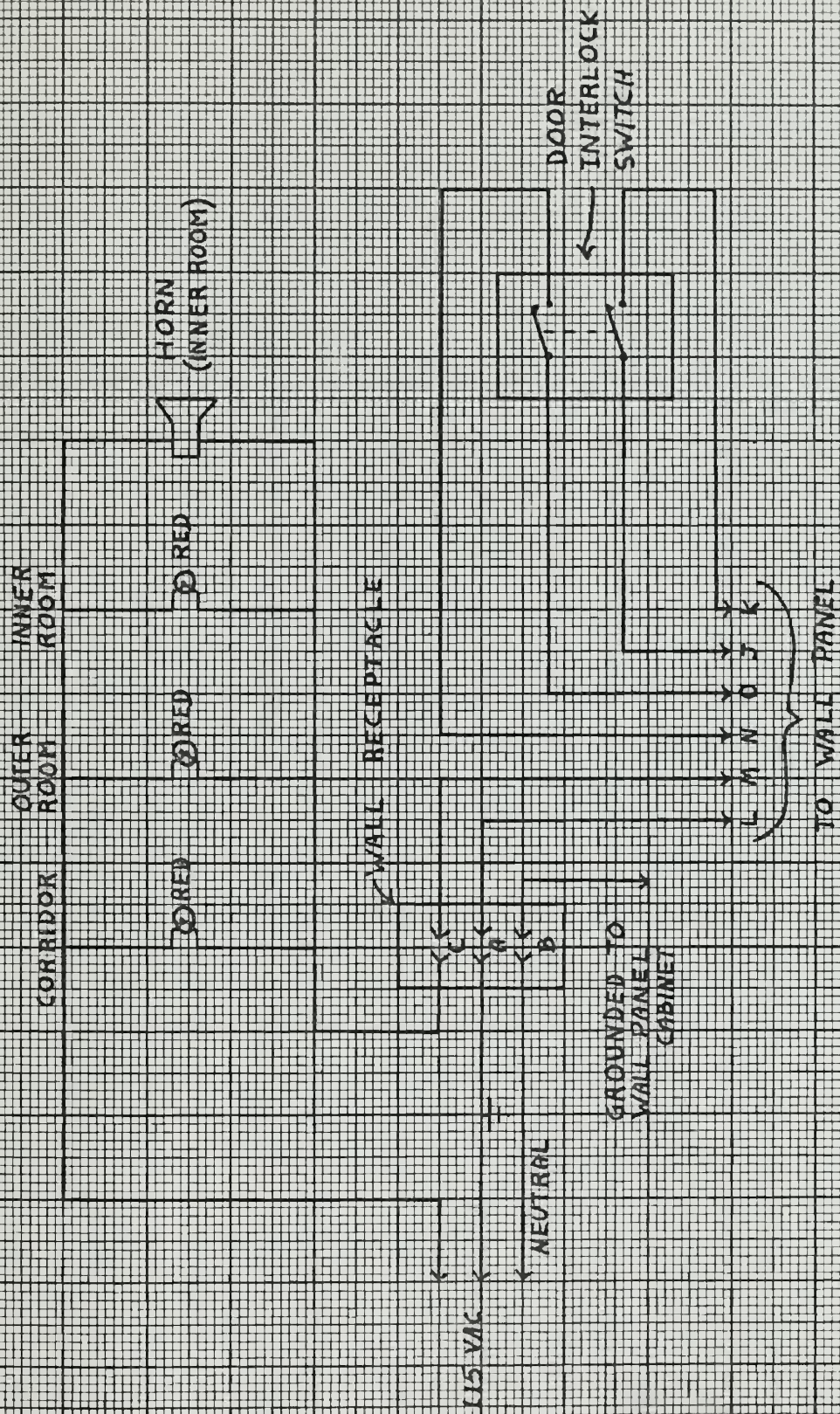
TO INTERLOCK AND WARNING CIRCUIT

RUBBER GROMMETS



BLAST CHAMBER WALL PANEL

FIGURE 2.4

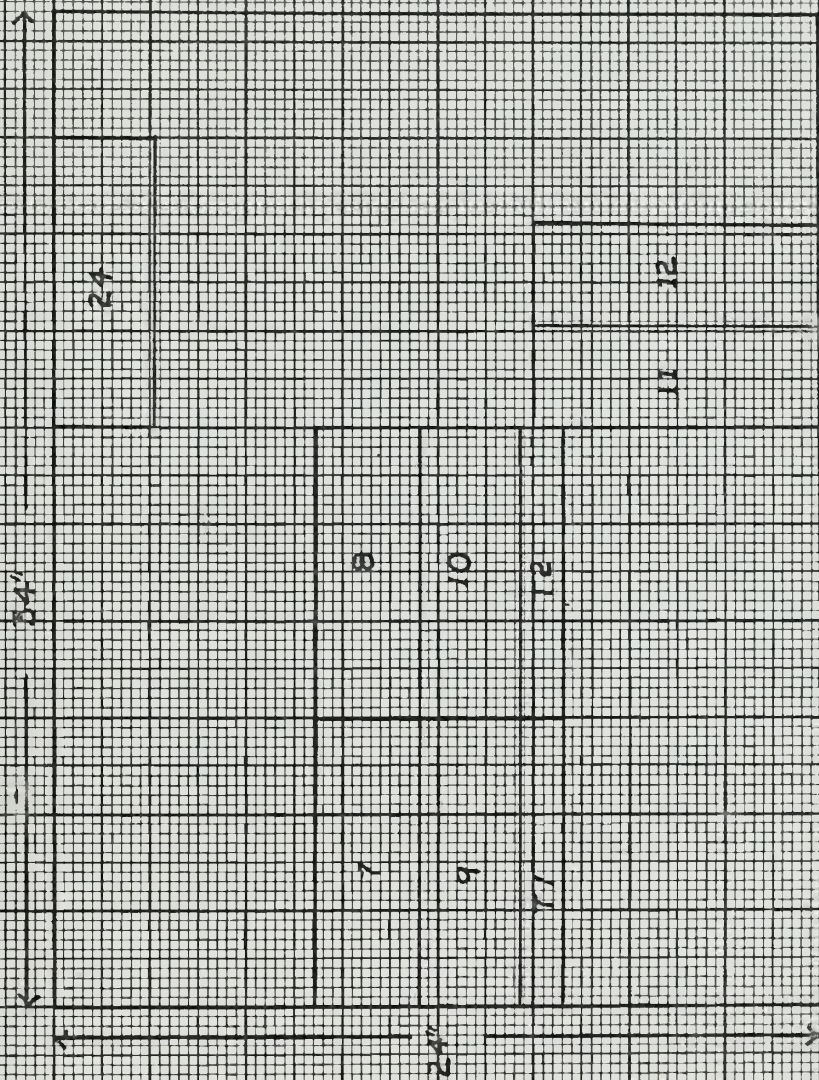


INTERLOCK & WARNING CIRCUIT
FIGURE 25

A coordinate plane with x and y axes. The x-axis is labeled from 26 to 32, and the y-axis is labeled from 24 to 32. A point is plotted at (28, 28).

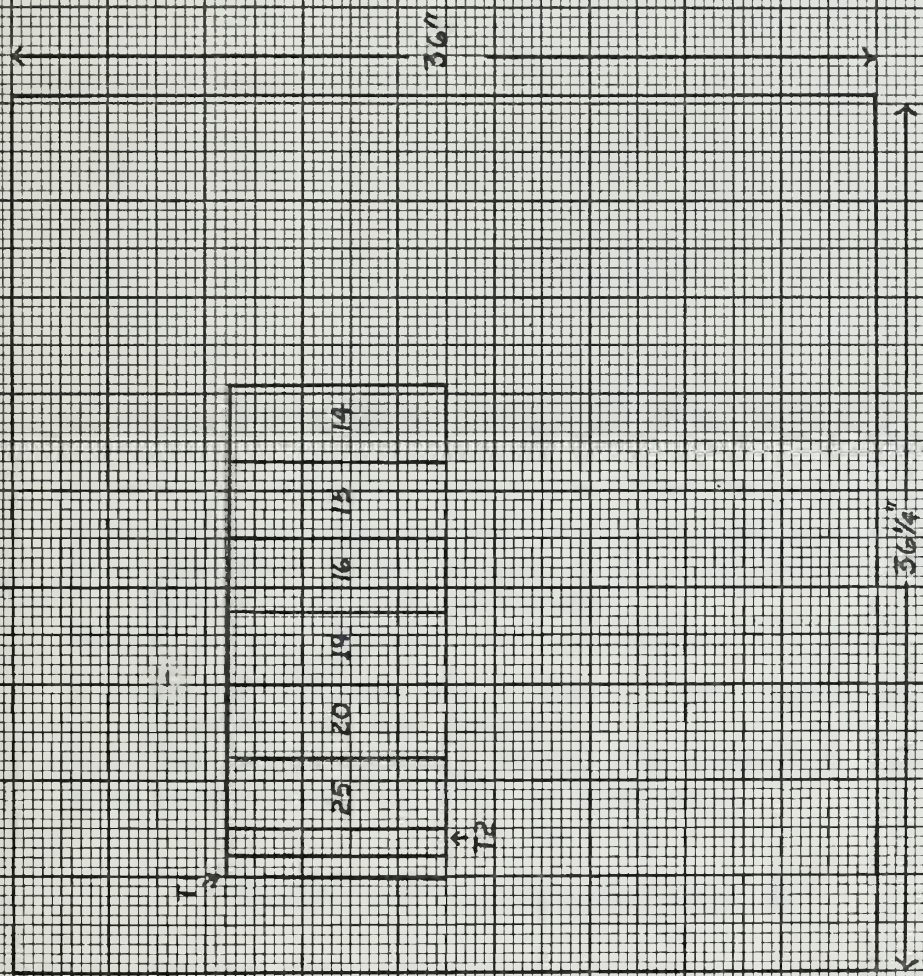


FIGURE 26



12 GAGE PLATE

FIGURE 27



14 GAGE PLATE

FIGURE 28

APPENDIX H

Initial Velocity Calculation

The maximum potential energy attained by the pendulum during a test can be calculated knowing the pendulum swing. By equating the maximum potential energy to the maximum kinetic energy, the velocity of the pendulum at the center of the swing can be calculated. A momentum balance between the plate specimen and the pendulum will yield the initial velocity of the plate. The initial velocity of the plate is a direct measure of the impulse or energy imparted to the plate by the explosive.

The equation used to calculate the initial velocity was taken from page 19 of reference [8] .

$$V_0 = \frac{\sqrt{2g (WD^2 + W_s L^2)} D (1 - \cos \theta) W}{W_s L}$$

- W = Total weight of the pendulum and specimen.
- D = Distance from the pivot to the center of gravity of the pendulum.
- W_s = Specimen weight (not including the part in the clamps).
- L = Distance from the pivot to the center of gravity of the plate.
- θ = The angle through which the pendulum swings.
- g = Acceleration due to gravity.

Sample Calculation Specimen 2

$$W_s = \rho \cdot X \cdot L_p \cdot t = .2789 (2.977) (5.046) (.1729) \\ = .724 \text{ lbs.}$$

$$\theta = \frac{S}{R} \text{ radius} = \frac{180 S}{\pi R} \text{ degrees} \\ = \frac{180 (7.525)}{133.4 \pi} = 3.23 \text{ degrees}$$

$$\cos \phi = .9984$$

$$L = 128.8 \text{ in}$$

$$D = 128.2 \text{ in}$$

$$W = 76.5 \text{ lbs}$$

$$V_0 = \frac{[12(64.4)\{76.5(128.2)^2 + .724(128.8)^2\}(128.2)(.0015)(76.5)]^{1/2}}{.724(128.8)}$$

$$V_0 = \frac{1.19 \times 10^5}{93.2}$$

$$V_0 = 1275 \text{ in/sec}$$

REFERENCES

1. P. Symonds and T. Mentel, "Impulsive Loading of Plastic Beams with Axial Constraints", Journal of the Mechanics and Physics of Solids, vol. 6, 1958, p. 186.
2. S. Bodner and P. Symonds, "Experimental and Theoretical Investigation of the Plastic Deformation of Cantilever Beams Subjected to Impulsive Loading", Journal of Applied Mechanics, vol. 29, Trans. ASME, vol. 84, Series E, December 1962, p. 719.
3. N. Jones, "Finite Deflections of a Simply Supported Rigid-Plastic Annular Plate Loaded Dynamically", Int. J. Solids Structures, vol. 4, 1968, p. 593.
4. J. S. Humphreys, "Plastic Deformations of Impulsively Loaded Straight Clamped Beam", Journal of Applied Mechanics, vol. 32, Trans. ASME, vol. 87, Series E, 1965, p. 7.
5. A. L. Florence and L. D. Firth, "Rigid-Plastic Beams Under Uniformly Distributed Impulses", Journal of Applied Mechanics, September 1965, p. 481.
6. N. Jones, "Influence of Strain-Hardening and Strain-Rate Sensitivity on the Permanent Deformations of Impulsively Loaded Rigid-Plastic Beams", Int. Journal Mech. Sci., vol. 9, 1967, p. 777.
7. N. Jones, "An Experimental Study into the Behavior of Beams Subjected to Large Dynamic Loads", not yet published.
8. W. Goldsmith, Impact, London: Edward Arnold, 1960.

ACKNOWLEDGMENT

The author would like to take this opportunity to express his appreciation for the assistance he received from John Leech, Fred Merlis and Oscar Wallin of the Aero-elastics Laboratory. Their technical and material aid in building and assembling the apparatus was invaluable.

thesG783

Finite deflections of impulsively loaded



3 2768 002 13924 8

DUDLEY KNOX LIBRARY